https://doi.org/10.5194/hess-2022-261
Preprint. Discussion started: 2 August 2022

Hydrology and Earth System Sciences
Open Access
EGU
Discussions

From soil water monitoring data to vadose zone water fluxes: a comprehensive example of reverse hydrology

Marleen Schübl[1], Giuseppe Brunetti[1], Gabriele Fuchs[2], and Christine Stumpp[1]

[1]University of Natural Resources and Life Sciences, Vienna, Department of Water, Atmosphere and Environment, Institute of Soil Physics and Rural Water Management, Muthgasse 18, 1190 Vienna, Austria
[2]Federal Ministry of Agriculture, Regions and Tourism (BMLRT), Division I/3: Department of Water Resources, Marxergasse 2, 1030 Vienna, Austria

Correspondence: Marleen Schübl (marleen.schuebl@boku.ac.at)

Abstract. Groundwater recharge is a key component of the hydrological cycle, yet its direct measurement is complex and often difficult to achieve. An alternative is its inverse estimation through a combination of numerical models and transient observations from distributed soil water monitoring stations. However, an often neglected aspect of this approach is the effect of model predictive uncertainty on simulated water fluxes. In this study, we made use of long-term soil water content measurements at 14 locations from the Austrian soil water monitoring program to quantify and compare local, potential groundwater recharge rates and their temporal variability. Observations were coupled with a Bayesian probabilistic framework to calibrate the model HYDRUS-1D and assess the effect of model predictive uncertainty on long-term simulated recharge fluxes. Estimated annual potential recharge rates ranged from 44 mm a^{-1} to 1319 mm a^{-1} with a relative uncertainty (95% interquantile range/median) in the estimation between 1-39%. Recharge rates decreased longitudinally, with high rates and lower seasonality at western sites and low rates with high seasonality and extended periods without recharge at the southeastern and eastern sites of Austria. Higher recharge rates and lower actual evapotranspiration were related to sandy soils; however, climatic factors had a stronger influence on estimated potential groundwater recharge than soil properties, underscoring the vulnerability of groundwater recharge to the effects of climate change.

1 Introduction

Groundwater is the largest reservoir of liquid freshwater on earth and one of the most important sources of drinking and irrigation water. Under changing climatic conditions with extremes occurring more frequently and intensely, the strategic importance of groundwater for global water and food security is expected to further increase (Taylor et al., 2013). In some countries, such as Austria, groundwater including spring water is the most important water resource, making up 100% of the water supply (Vogel, 2001). The major limitation for sustainable groundwater use is recharge, which represents the maximum amount of water that may be withdrawn from an aquifer without depleting it. This makes it a crucial variable for groundwater resource management (Moeck et al., 2020; Taylor et al., 2013). A large portion of groundwater recharge comes from water infiltrating soil and flowing through the vadose zone towards the water table (Döll and Fiedler, 2008; Nolan et al., 2007). Infiltration capacity, root water uptake and evaporation from the upper soil layers determine the net amount of water which is transported into the deeper vadose zone, following the gradient in matric potential and gravity (Vereecken et al., 2008). Water flow through the vadose zone is supposed to have a major influence on the process of groundwater recharge even at karst mountain sites (Berthelin et al., 2020; Hartmann et al., 2014; Kaminsky et al., 2021; Neukum et al., 2008).

The quantification of recharge is complicated by temporal and spatial variability and by the fact that direct measurements are difficult (Moeck et al., 2020, 2018; Nolan et al., 2007; Scanlon et al., 2002). Lysimeters are the only means to obtaining local measurements of seepage flow, which can be considered a good indicator of groundwater recharge (Moeck et al., 2020, 2018; Seneviratne et al., 2012; von Freyberg et al., 2015). However, their appropriate set up is difficult without introducing a bias in the hydrological processes (Barkle et al., 2011; Groh et al., 2016; Pütz et al., 2018; Stumpp et al., 2012). Furthermore, the operation and maintenance of lysimeters is expensive, which is why long-term lysimeter measurements are scarce (Nolz et al., 2016; von Freyberg et al., 2015). Among the most widely used alternatives for recharge estimation are methods based on artificial and environmental tracer experiments (e.g., Boumaiza et al., 2020; Chesnaux and Stumpp, 2018; Koeniger et al., 2016) and groundwater table fluctuations (Moeck et al., 2020; Collenteur et al., 2021). Common water table fluctuation methods, however, face some limitations in reflecting and predicting the actual recharge process (Collenteur et al., 2021; Healy and Cook, 2002).

Moeck et al. (2020) collected and investigated a global scale data set of natural groundwater recharge rates where, however, recharge rates from high altitudes were underrepresented. For mountain sites in particular, there is a lack of reported groundwater recharge rates (Bresciani et al., 2018; Moeck et al., 2020). A limited number of studies report local or regional recharge rates based on different modeling approaches using field measurements, such as groundwater levels and river discharge, or available information on vegetation and subsurface, and assess controlling factors on groundwater recharge (e.g., Barron et al., 2012; Collenteur et al., 2021; Hartmann et al., 2017; Keese et al., 2005; Neukum and Azzam, 2012).

An alternative is the inverse estimation of recharge fluxes through the unsaturated zone by calibrating vadose zone hydrological models against transient observations (e.g., soil water content and pressure head). Over the last decades, numerical modeling of soil water fluxes has been applied and improved, resulting in today's state of the art soil models with an implementation of the Richards Equation for simulating the transport of water through the soil, considering heat and energy balances and accounting for relevant processes such as plant water uptake and snow hydrology (Šimůnek et al., 2016, 2003; Vereecken et al., 2016).

The core of this modeling approach is generally the inverse estimation of hydraulically relevant parameters, such as Soil Hydraulic Parameters (SHPs) (e.g., Van Genuchten, 1980). The use of field measurements guarantees a higher generalizability of estimated parameters compared to small scale measurements of soil samples in the laboratory (Dyck and Kachanoski, 2010; Groh et al., 2018; Stumpp et al., 2012; Vereecken et al., 2008; Vrugt et al., 2008; Wöhling et al., 2008). Several studies have evaluated the use of vadose zone measurements for the inverse estimation of effective SHPs and the reliable prediction of recharge fluxes (Durner et al., 2008; Groh et al., 2018; Schelle et al., 2012). However, inverse parameter estimation is often treated as an optimization problem aiming at a unique solution, which neglects the uncertainty which is fundamentally associated with parameter identification. Uncertainties originate from different error sources including model input and forcing data, the initial and boundary conditions, the model structure, heterogeneity and scale effects (Beven, 2006; Vereecken et al.,

https://doi.org/10.5194/hess-2022-261
Preprint. Discussion started: 2 August 2022

Hydrology and Earth System Sciences Discussions
Open Access EGU

2016). Further, the quality and scope of calibration data affects the uncertainty in parameter estimation. It is important not to neglect uncertainties related to the model calibration as they can lead to uncertain or even failing predictions (Finsterle, 2015; Vrugt and Sadegh, 2013). The emergence of computationally efficient algorithms makes it possible to deal with uncertainties in a statistically rigorous way based on the Bayesian approach to statistics (e.g., Brunetti et al., 2019; Scharnagl et al., 2011; Wöhling et al., 2008). This approach relies on the idea of integrating a priori knowledge of the system in the statistical inference, to combine it with observed data in order to derive the posterior probability distribution of parameter values, which can be used to quantify model uncertainty.

In combination with a soil hydraulic model, an efficient algorithm is needed to compute posterior distributions with an iterative Monte Carlo approach and to allow for a clear convergence in a reasonable amount of time. Skilling (2006) introduced Nested Sampling as an efficient Monte Carlo method to estimate the integral of the Bayesian evidence, the denominator of the Bayes Theorem, and obtain posterior distributions as a side product. Its efficiency has been further increased with ellipsoidal Nested Sampling (Mukherjee et al., 2006). Finally, ellipsoidal rejection sampling, as proposed by Feroz et al. (2009) with the MULTINEST algorithm, is able to account efficiently for multimodal posterior distributions. A Bayesian statistical framework using a Nested Sampling approach in combination with a physically based soil water model and soil water monitoring measurements thus provides a powerful tool for a comprehensive characterization of the vadose zone at individual sites and the estimation of local water balances, including an assessment of the model uncertainties.

In this study, we made use of long-term volumetric soil water content measurements at 14 different locations from the Austria wide soil water monitoring program and integrated them in a Bayesian probabilistic framework with the MULTINEST algorithm to calibrate the hydrological model HYDRUS-1D at each location. We used this approach to account for the uncertainties inherently associated with the inverse parameter estimation, and we simultaneously assessed and propagated the model predictive uncertainty in simulated local potential groundwater recharge rates. All sites were modelled with the same approach on a similar data basis supporting comparability of the results. Site properties included a variety of soils and climatic conditions which allowed to investigate factors which influence the long-term soil water balances and temporal variability of potential groundwater recharge.

2 Material and methods

2.1 Austrian soil water monitoring program

The locations of 14 Austrian soil water monitoring sites are shown in Fig. 1(a). Figure 1(b) gives an overview over soil types according to the digital soil map of Austria (BFW, 2016). Figures 1(c) and 1(d) show long-term annual areal precipitation and actual evapotranspiration estimates (modified from Kling et al. (2007b) and Kling et al. (2007a), respectively. According to texture information (ÖNORM L 1050), the soil types at the measurement sites vary between sand and silt loam/loamy silt (11 – 88% sand, 12 – 75 % silt, and 0 – 32% clay). Details on altitude, geo-coordinates, soil textures, and measurement depths are given in the Appendix (Table A1). Zettersfeld, Gschlössboden and Sillianberger Alm are on the sub-alpine level in the southwest of Austria, characterized by high contents in organic matter, coarse soil texture and/or high skeleton fraction;

Leutasch, Achenkirch, Gumpenstein and Aichfeld-Murboden are at the montane level from western to central Austria with soil textures ranging between sand and loam; Pettenbach, Elsbethen and Lauterach are located at the foothill zone in western to central Austria with soil textures ranging from loam to loamy silt; Kalsdorf, Schalladorf, Lobau and Frauenkirchen are situated in the southern and eastern lowlands with sandy to loamy soil textures. Locations included in this study are horizontally even at the plot scale, and usually consisting of uncultivated grassland. In contrast, cultivation of alternating crops was carried out at the location Pettenbach, where details on the crop cover for calibration and validation periods were obtained from technical reports provided by the Upper Austrian Government (Land OÖ, 2013, 2014).

Long-term field measurements of volumetric soil water content, measured with Time Domain or Frequency Domain Reflectometry (TDR/FDR) over several years, partly since 1996, are carried out within the Austrian Soil Water Monitoring Program of the Federal Ministry of Agriculture, Regions and Tourism (BMLRT). Under this program, continuous measurements are conducted at various depth levels of soil profiles with the aim of providing standardized and quality assured measurement data. For inverse parameter estimation in this study, we selected calibration periods of around six months with sufficiently complete and plausible soil water content measurement series from two to five depth levels (Table A1 in the Appendix) and aggregated the data to a daily resolution. The program also offers composite matric potential measurements from tensiometers and gypsum blocks. The discontinuity of the data complicates the modeling and analysis, which is why they have not been used in this study. Further, the winter season was excluded from the calibration periods to avoid the simulation of snow. This procedure allowed to reduce computational cost and numerical sensitivity of the simulations which often lead to non-convergence or delayed convergence of the sampling algorithm in the Bayesian analysis (described in Sect. 2.3). Validation periods were chosen to provide one year or more of continuous, plausible data. Snow hydrology was simulated for the model validation, as described in Sect. 2.2. Details on calibration and validation periods are summarized in Table A2. Several locations were equipped with lysimeters: At Leutasch and Pettenbach, in situ soil water content measurements were directly obtained from lysimeter set ups; in Gumpenstein, soil water content measurements were obtained from a soil profile next to a lysimeter cluster which provided long-term seepage measurements. Lysimeter measurements from Leutasch and Gumpenstein were used for additional validation of recharge rates.

2.2 Modelling theory

2.2.1 Water flow and root water uptake

The mechanistic model HYDRUS-1D (Šimůnek et al., 2016) was used to simulate water flow in the vadose zone profiles. HYDRUS-1D is a finite element model that numerically solves the one-dimensional Richards equation [Eq. (1)]

$$\frac{\delta\theta}{\delta t} = \frac{\delta}{\delta z}\left[K(h)\left(\frac{\delta h}{\delta z}+1\right)\right] - S(h) \tag{1}$$

where $\theta[L^3L^{-3}]$ is the volumetric water content, $t[T]$ is the time variable, $z[L]$ is a vertical coordinate, $K(h)[LT^{-1}]$ is the

https://doi.org/10.5194/hess-2022-261
Preprint. Discussion started: 2 August 2022

Hydrology and Earth System Sciences
Open Access
Discussions

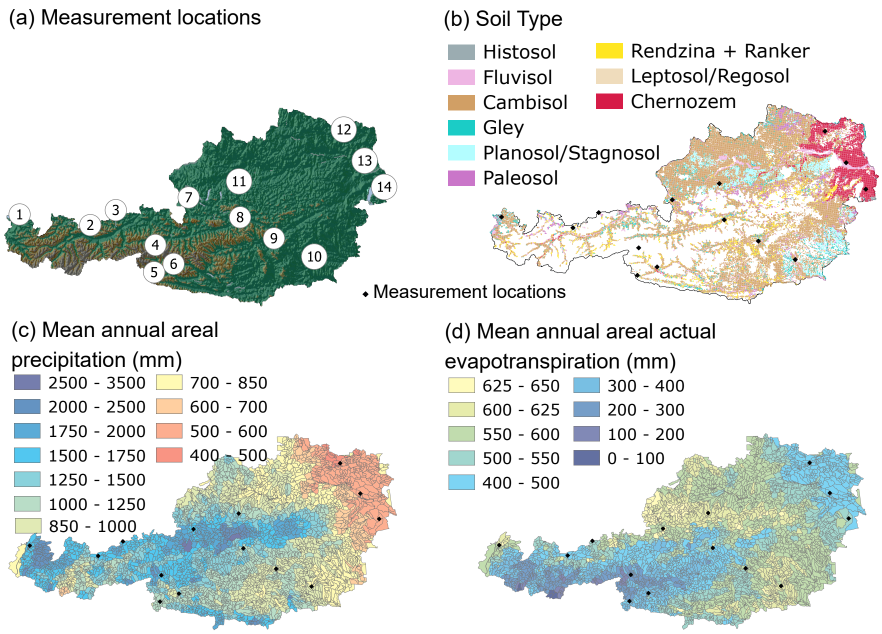

Figure 1. (a) Locations of 14 monitoring sites in Austria (1) Lauterach, (2) Leutasch, (3) Achenkirch, (4) Gschlössboden, (5) Sillianberger Alm, (6) Zettersfeld, (7) Elsbethen, (8) Gumpenstein, (9) Aichfeld-Murboden, (10) Kalsdorf, (11) Pettenbach, (12) Schalladorf, (13) Lobau, (14) Frauenkirchen; (b) Soil map data basis: Digital soil map of Austria, 1km raster, Federal Forest Research Center (BFW, 2016); (c) Hydrological Atlas of Austria (HAO) mean areal annual precipitation (Kling et al., 2007b); (d) HAO mean areal annual actual evapotranspiration (Kling et al., 2007a); Maps from the HAO where compiled using QGIS (QGIS Development Team, 2022).

unsaturated hydraulic conductivity function and $h[L]$ is the pressure head. S is a sink term accounting for water uptake by plant roots. The unimodal Van Genuchten-Mualem (VGM) model described the soil hydraulic properties, namely the soil water retention curve [Eq. (2)], and the unsaturated hydraulic conductivity [Eq. (3)]:

$$\theta(h) = \begin{cases} \theta_r + \frac{\theta_s - \theta_r}{(1+(|\alpha h|)^n)^m}, & h < 0 \\ \theta_s, & h \geq 0 \end{cases} \tag{2}$$

$$K(h) = K_s S_e^l \left[1 - \left(1 - S_e^{1/m}\right)^m\right]^2 \tag{3}$$

$$m = 1 - 1/n, n > 1 \tag{4}$$

$$S_e = \frac{\theta - \theta_r}{\theta_s - \theta_r} \tag{5}$$

https://doi.org/10.5194/hess-2022-261
Preprint. Discussion started: 2 August 2022

Hydrology and Earth System Sciences
Open Access
Discussions

where $\theta_r[L^3L^{-3}]$ is the residual water content, $\theta_s][L^3L^{-3}]$ is the saturated water content, $\alpha[L^{-1}]$, $n[-]$ and $m[-]$ are van-Genuchten shape parameters, with the relation given in Eq. (4), Se [-] is the effective saturation (defined in Eq. (5)) and $l[L]$ is a pore connectivity parameter. The unimodal VGM model was successfully used in several studies to parameterize the hydraulic behavior of variably saturated soils (e.g., Brunetti et al., 2020b; Dettmann et al., 2014; Lambot et al., 2002). It has been shown to become more inconsistent in the clay range of soil textures (Fuentes et al., 1992); however, this limitation does not affect any soils in the framework of this study and was thus employed for all sites. The sink term for the simulation of plant water uptake is implemented according to Eq. (6) (Feddes et al., 1978), where $r_d[L]$ is the root depth, $T_p[L]$ is the potential transpiration and α(h) is a prescribed water stress response function depending on the crop type. The crop parameterization for the sites in this study used the default values for grass cover (Taylor et al., 1972), except for the Pettenbach calibration with maize parameterization according to Wesseling et al. (1991).

$$S(h) = \alpha(h)\frac{1}{r_d}T_p \tag{6}$$

The model domain was set up from soil surface to 1.5 m depth at all sites and two different soil materials were defined for the upper soil (including 20 cm root zone) and the lower soil, respectively. The depths of the soil layers are given in the Appendix in Table A3. In this study, we define the point at which percolating water is expected to contribute to groundwater recharge as the amount of water that arrives at the bottom of the area at a depth of 1.5 m, well below the root zone. It is assumed that water arriving at this depth will not be subject to further loss mechanisms and so will reach the water table (Heppner et al., 2007). However, since the point where water actually reaches the water table remains unknown, the estimation with this approach can be referred to as potential recharge (Scanlon et al., 2002).

Daily time-steps were used in all simulations, for variable boundary conditions as well as simulated soil water content and water fluxes. Meteorological data for the sites, including precipitation, solar radiation, sunshine duration, wind speed, and relative humidity, were obtained from the Central Institution for Meteorology and Geodynamics (ZAMG), Austria. The potential evapotranspiration ET_0 was calculated with the FAO Penman-Monteith method according to Allen et al. (1998). At the upper boundary of the model domain, an "atmospheric", "zero-ponding" boundary condition was specified, where an equilibrium is prescribed between the soil surface pressure and atmospheric water vapor pressure when the evaporative demand exceeds the soil evaporation capacity, and where the pressure at the soil surface is set to zero when both infiltration and surface runoff occur. The lower boundary of the model domain was set to seepage face for the lysimeter sites (Leutasch and Pettenbach) and to free-drainage for all other sites during the calibration period. For the simulation of long-term potential recharge rates, the lower boundary condition at all sites was set to free-drainage in order to reflect natural conditions with a water table far below the model domain. To improve comparability of long-term simulations at the sites, a grass reference was used with the calibrated Pettenbach model to simulate long-term groundwater recharge. Long-term simulations comprised the entire period of available soil water and meteorological data. For the location Achenkirch, only two years of meteorological data (2017-2018) were available.

For model validation and long-term simulations, snow accumulation and snow melt was accounted for in HYDRUS-1D. The model treats any precipitation falling at a temperature below -2°C as snow and any precipitation above +2°C as liquid, assuming a linear transition between -2°C and +2°C. A 0.4 snow sublimation constant was used for the reduction of potential evaporation from snow and the simulation of snow melt at temperatures above 0°C used a constant of 0.43 cm day $^{-1}$ °C^{-1}.

2.2.2 Bayesian analysis

The Bayes Theorem (Eq. 7) is the basis for the estimation of parameter posterior distributions which are used for quantification of model parameter uncertainties after calibration. Here, $P(\Omega \mid D, M)$ is the posterior distribution of the model parameters (Ω), given the data (D) and the model (M), $P(D \mid M, \Omega)$ is the data likelihood, $P(\Omega \mid M)$ is the prior parameter distribution and $P(D|M)$ is the marginal likelihood or Bayesian model evidence (BME). Measurement errors are assumed to be independent, homoscedastic, and normally distributed, thus leading to a Gaussian likelihood function [Eq. (8)], where σ is the standard deviation in the measurement error, $M_i(\Omega)$ is the model realization and $\tilde{y}_i$ is the corresponding observed data.

$$P(\Omega \mid D, M) = \frac{P(D \mid M, \Omega) P(\Omega \mid M)}{P(D \mid M)} \tag{7}$$

$$L(\Omega) = \prod_{i=1}^{k} \frac{1}{\sqrt{2\pi\sigma^2}} \exp\left[-\frac{1}{2}\sigma^2 \left(M_i(\Omega) - \tilde{y}_i\right)^2 \right] \tag{8}$$

At all 14 locations, 10 soil hydraulic parameters (SHPs) (residual and saturated water content parameters θ_r and θ_s, shape parameters α and n, and the saturated hydraulic conductivity parameter K_s, for two soil layers, respectively) were estimated per site. The pore connectivity parameter l was fixed to 0.5 according to Mualem (1976). Together with the SHPs, the standard deviations of the measurement errors were estimated in the Bayesian inference. Uniform prior distributions were assumed for all parameters. Their ranges were established based on texture information, literature review, and preliminary testing to prevent cutting off the posterior distributions. Final ranges are given in the Appendix in Table A3.

The implementation of the Bayesian approach in a numerical framework can become challenging for non-linear models such as the model used here. The Nested Sampling algorithm as proposed by Skilling (2006) has been used successfully for parameter estimation and uncertainty quantification in studies with non-linear hydrological or biogeochemical models (Brunetti et al., 2020a; Elsheikh et al., 2013). It is an efficient Monte Carlo method which estimates the Bayesian model evidence and calculates posterior distributions as a side product. It transforms the multi-dimensional integral of the Bayesian model evidence (BME) into a one-dimensional one, which is then solved iteratively, based on the evaluation and redistribution of a number of “live points” over the parameter space. Several improvements were implemented with the original algorithm such as the ellipsoidal rejection sampling scheme which is able to establish multiple posterior modes. This has been realized in

Hydrology and Earth System Sciences
Open Access
Discussions

the algorithm MULTINEST by Feroz et al. (2009). The algorithm has been shown to be well suited to multimodal distributions and moderately complex inverse problems with up to 20 parameters (Buchner, 2016; Feroz and Hobson, 2008). The algorithm is particularly suitable for our study because it offers a high level of efficiency for unimodal problems while also handling the possibility of multimodal posteriors. Further details on the algorithm can be found in Feroz et al. (2019, 2009), Feroz and Hobson (2008) and Mukherjee et al. (2006).

Here, we used a number of live points N=100 to sample the parameter space. This number has been shown to produce a reliable estimate of the BME integral (and therefore a satisfactory sampling of the parameter space) in a sensitivity analysis by Brunetti et al. (2020a, b) for similar models and dimensionalities. At each iteration of the algorithm, the current maximum likelihood sample point is multiplied with the remaining prior volume to estimate the maximum remaining volume of the BME integral. Sampling is then terminated according to a tolerance criterion, which defines when the remaining contribution from the current live points to the integral is considered to be small enough. At this point, it is expected, that the bulk of the posterior has been sampled sufficiently. The tolerance parameter in this study was set to 0.5. After successful model calibration, we used samples from the posterior distributions to propagate parameter uncertainty in the model for long-term simulations to quantify the resulting uncertainty in recharge simulations.

2.2.3 Statistical analysis

Simulations with the successfully calibrated models were used in a second step to perform a statistical analysis in order to characterize and describe the variability of groundwater recharge at the monitoring sites and to assess the influence of climatic, geographic and soil properties on potential groundwater recharge rates and their temporal variability. For this purpose, we used a Principle Component Analysis (PCA) and established clusters of sites with similar properties using Agglomerative Clustering (Pedregosa et al., 2011). In order to quantify the temporal variability in water balance components, we calculated the coefficients of variations (CVs) defined as the quotient of standard deviations between months within a year as measure for seasonal variability. Spearman's Rho correlations were used to identify predictor variables for potential groundwater recharge rates and temporal variability. Significance of correlations were evaluated at a 90% confidence level ($p<0.1$).

3 Results and discussion

3.1 Calibration and validation

The required number of iterations of the MULTINEST algorithm with models for all 14 locations ranged between 2595 and 5515 (4111 on average) until the termination criterion was satisfied (as described in Sect. 2.3), generally resulting in unimodal posterior parameter distributions. Median parameter estimates and estimated measurement errors including the 95% credible interval are given in Table 1 for upper and lower soil layers at the 14 sites. Figure 2(a) shows exemplarily for the location Gumpenstein the calibrated measurement error and median prediction of the volumetric soil water content for the upper and

https://doi.org/10.5194/hess-2022-261
Preprint. Discussion started: 2 August 2022

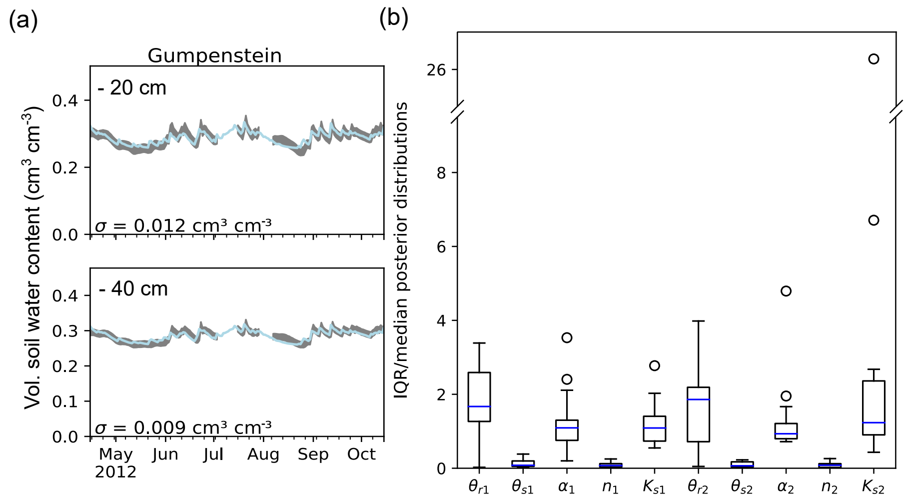

Figure 2. Inverse parameter estimation and uncertainty: (a) Gumpenstein calibration period with soil water content measurements (grey) from two depth levels including the calibrated measurement error σ, and prediction with median parameter estimates (blue); (b) Boxplots of estimated parameter uncertainties (index 1 for upper, index 2 for lower soil layer) from all 14 sites, as ratios between 95% interquantile range (IQR) and median estimates.

lower soil layer. Calibration plots for all 14 sites are shown in Fig. A1 in the Appendix. Uncertainty in the parameter estimation is summarized for all 14 sites in Fig. 2(b) as ratios between the 95% interquantile range (IQR) and the median estimate.

Median estimates for the VGM shape-parameters α and n varied between 0.001 – 0.945 cm^{-1} and 1.01 – 2.30, respectively, where α was < 0.01 cm^{-1} at most sites. Except for the high α estimates at Gschlössboden (α_1 = 0.945 cm^{-1}) and Lobau (α_1= 0.511 cm^{-1} and α_2 = 0.696 cm^{-1}), the VGM shape parameters fell well within the range of values predicted by the ROSETTA pedotransfer model (Schaap and Leij, 1998); high estimates for α and n coincided with a high reported fraction in sand. Median estimates for hydraulic conductivity parameters K_s ranged from 5–3863 cm d^{-1}, where high values were found for soils with high fractions in organic and stone content (Gschlössboden, Sillianberger Alm, Zettersfeld).

Generally, uncertainties in the estimation of the residual water content parameter θ_r and the saturated hydraulic conductivity parameter K_s for the sites were high, both for the upper and lower soil layers (IQR/median $\sim$ 26 for K_{s2} at Lauterach). The uncertainty in the shape parameter α was medium with a relative uncertainty (IQR/median) < 6 and mostly low absolute values in estimates and uncertainty ranges. The shape parameter n and the saturated water content parameter θ_s were identified with the highest precision (IQR/median<0.5).

The estimation of K_s has been frequently shown to be associated with high uncertainties (e.g., Baroni et al., 2010; Minasny and Field, 2005; Mishra et al., 1989). Brunetti et al. (2019) observed in the estimation of SHPs with remote sensing soil moisture data, that uncertainty in θ_r estimation was low whereas θ_s was highly uncertain. This was related to soil water content values being low in their study and mainly representative for unsaturated conditions. In this study, at the majority of the Austrian

https://doi.org/10.5194/hess-2022-261
Preprint. Discussion started: 2 August 2022

Hydrology and Earth System Sciences
Discussions

Table 1. Median estimates and 95 % credible interval of soil hydraulic parameters and measurement errors for upper (L1) and lower (L2) soil profiles.

Site		θ_r (cm^3 cm^{-3})	θ_s (cm^3 cm^{-3})	α (cm^{-1})	$n(-)$	K_s (cm d^{-1})	σ_{meas} (cm^3 cm^{-3})
Lauterach	L1	$0.134^{+0.062}_{-0.118}$	$0.425^{+0.019}_{-0.010}$	$0.002^{+0.002}_{-0.001}$	$1.34^{+0.19}_{-0.14}$	$133.9^{+65.2}_{-92.4}$	$0.024^{+0.002}_{-0.002}$
	L2	$0.068^{+0.094}_{-0.062}$	$0.390^{+0.072}_{-0.008}$	$0.006^{+0.028}_{-0.002}$	$1.19^{+0.09}_{-0.07}$	$5.3^{+165.0}_{-1.3}$	$0.027^{+0.003}_{-0.002}$
Leutasch	L1	$0.022^{+0.046}_{-0.021}$	$0.462^{+0.028}_{-0.067}$	$0.006^{+0.004}_{-0.002}$	$1.20^{+0.05}_{-0.06}$	$667.3^{+290.3}_{-339.2}$	$0.031^{+0.002}_{-0.002}$
	L2	$0.096^{+0.002}_{-0.003}$	$0.160^{+0.010}_{-0.009}$	$0.005^{+0.003}_{-0.002}$	$2.30^{+0.33}_{-0.27}$	$770.1^{+219.1}_{-272.0}$	$0.011^{+0.000}_{-0.001}$
Achenkirch	L1	$0.023^{+0.054}_{-0.021}$	$0.570^{+0.025}_{-0.020}$	$0.001^{+0.001}_{-0.000}$	$1.13^{+0.01}_{-0.02}$	$776.3^{+207.2}_{-333.4}$	$0.048^{+0.003}_{-0.004}$
	L2	$0.001^{+0.001}_{-0.001}$	$0.197^{+0.002}_{-0.003}$	$0.004^{+0.002}_{-0.001}$	$1.09^{+0.01}_{-0.01}$	$1843.8^{+1.011.6}_{-708.7}$	$0.011^{+0.000}_{-0.000}$
Gschlössboden	L1	$0.050^{+0.000}_{-0.001}$	$0.278^{+0.047}_{-0.025}$	$0.945^{+0.053}_{-0.126}$	$2.25^{+0.27}_{-0.07}$	$839.0^{+605.4}_{-284.6}$	$0.021^{+0.001}_{-0.001}$
	L2	$0.005^{+0.006}_{-0.005}$	$0.320^{+0.023}_{-0.046}$	$0.002^{+0.003}_{-0.001}$	$2.04^{+0.19}_{-0.17}$	$2320.5^{+293.5}_{-999.0}$	$0.009^{+0.001}_{-0.001}$
Sillianberger	L1	$0.143^{+0.052}_{-0.093}$	$0.536^{+0.042}_{-0.051}$	$0.006^{+0.009}_{-0.004}$	$1.12^{+0.03}_{-0.02}$	$3098.7^{+1769.1}_{-2043.5}$	$0.030^{+0.002}_{-0.002}$
Alm	L2	$0.189^{+0.010}_{-0.040}$	$0.535^{+0.022}_{-0.016}$	$0.002^{+0.001}_{-0.001}$	$1.11^{+0.02}_{-0.01}$	$3863.4^{+1034.2}_{-2520.3}$	$0.023^{+0.002}_{-0.002}$
Zettersfeld	L1	$0.082^{+0.061}_{-0.047}$	$0.583^{+0.015}_{-0.012}$	$0.060^{+0.228}_{-0.027}$	$1.09^{+0.02}_{-0.02}$	$562.0^{+1194.2}_{-290.5}$	$0.030^{+0.002}_{-0.002}$
	L2	$0.019^{+0.022}_{-0.017}$	$0.256^{+0.009}_{-0.010}$	$0.001^{+0.001}_{-0.000}$	$1.09^{+0.02}_{-0.01}$	$3344.6^{+1061.8}_{-1040.8}$	$0.007^{+0.000}_{-0.001}$
Elsbethen	L1	$0.105^{+0.082}_{-0.082}$	$0.453^{+0.012}_{-0.006}$	$0.001^{+0.001}_{-0.000}$	$1.13^{+0.05}_{-0.03}$	$144.8^{+52.7}_{-87.3}$	$0.013^{+0.001}_{-0.001}$
	L2	$0.031^{+0.074}_{-0.028}$	$0.408^{+0.020}_{-0.010}$	$0.001^{+0.001}_{-0.000}$	$1.16^{+0.06}_{-0.03}$	$18.3^{+37.7}_{-8.5}$	$0.019^{+0.002}_{-0.002}$
Gumpenstein	L1	$0.051^{+0.027}_{-0.038}$	$0.375^{+0.014}_{-0.010}$	$0.003^{+0.001}_{-0.001}$	$1.08^{+0.01}_{-0.01}$	$392.1^{+97.6}_{-111.6}$	$0.012^{+0.001}_{-0.001}$
	L2	$0.067^{+0.034}_{-0.050}$	$0.333^{+0.008}_{-0.007}$	$0.001^{+0.001}_{-0.001}$	$1.08^{+0.01}_{-0.02}$	$214.2^{+172.5}_{-105.6}$	$0.009^{+0.001}_{-0.001}$
Aichfeld-	L1	$0.214^{+0.035}_{-0.052}$	$0.391^{+0.010}_{-0.004}$	$0.026^{+0.048}_{-0.012}$	$1.06^{+0.02}_{-0.02}$	$856.3^{+135.1}_{-294.8}$	$0.021^{+0.001}_{-0.001}$
Murboden	L2	$0.100^{+0.015}_{-0.015}$	$0.245^{+0.023}_{-0.017}$	$0.661^{+0.299}_{-0.264}$	$1.23^{+0.08}_{-0.05}$	$57.0^{+77.1}_{-33.8}$	$0.008^{+0.001}_{-0.000}$
Kalsdorf	L1	$0.036^{+0.044}_{-0.030}$	$0.448^{+0.080}_{-0.078}$	$0.011^{+0.008}_{-0.006}$	$1.46^{+0.24}_{-0.12}$	$486.9^{+469.1}_{-367.3}$	$0.043^{+0.004}_{-0.003}$
	L2	$0.017^{+0.016}_{-0.016}$	$0.309^{+0.024}_{-0.009}$	$0.033^{+0.020}_{-0.011}$	$1.50^{+0.14}_{-0.08}$	$867.4^{+130.4}_{-301.3}$	$0.016^{+0.002}_{-0.001}$
Pettenbach	L1	$0.063^{+0.108}_{-0.057}$	$0.387^{+0.005}_{-0.006}$	$0.001^{+0.001}_{-0.000}$	$1.15^{+0.06}_{-0.04}$	$245.3^{+239.7}_{-189.9}$	$0.036^{+0.004}_{-0.002}$
	L2	$0.163^{+0.061}_{-0.068}$	$0.405^{+0.006}_{-0.007}$	$0.516^{+0.467}_{-0.421}$	$1.03^{+0.01}_{-0.01}$	$19.6^{+99.8}_{-16.2}$	$0.012^{+0.001}_{-0.001}$
Schalladorf	L1	$0.013^{+0.033}_{-0.012}$	$0.455^{+0.039}_{-0.034}$	$0.011^{+0.007}_{-0.005}$	$1.28^{+0.06}_{-0.05}$	$17.1^{+27.2}_{-10.7}$	$0.023^{+0.002}_{-0.001}$
	L2	$0.049^{+0.066}_{-0.046}$	$0.395^{+0.005}_{-0.002}$	$0.001^{+0.001}_{-0.000}$	$1.22^{+0.06}_{-0.07}$	$1.5^{+1.2}_{-0.5}$	$0.005^{+0.001}_{-0.000}$
Lobau	L1	$0.006^{+0.013}_{-0.006}$	$0.723^{+0.019}_{-0.032}$	$0.511^{+0.266}_{-0.106}$	$1.18^{+0.01}_{-0.01}$	$684.5^{+201.0}_{-196.4}$	$0.044^{+0.002}_{-0.002}$
	L2	$0.173^{+0.052}_{-0.055}$	$0.378^{+0.004}_{-0.004}$	$0.696^{+0.268}_{-0.304}$	$1.01^{+0.01}_{-0.00}$	$262.0^{+491.5}_{-149.0}$	$0.004^{+0.000}_{-0.000}$
Frauenkirchen	L1	$0.049^{+0.045}_{-0.047}$	$0.489^{+0.052}_{-0.043}$	$0.001^{+0.001}_{-0.000}$	$1.46^{+0.12}_{-0.10}$	$333.4^{+150.2}_{-212.4}$	$0.0299^{+0.003}_{-0.003}$
	L2	$0.008^{+0.012}_{-0.007}$	$0.359^{+0.043}_{-0.031}$	$0.002^{+0.001}_{-0.000}$	$1.32^{+0.07}_{-0.03}$	$269.8^{+195.1}_{-117.5}$	$0.019^{+0.002}_{-0.001}$

locations, soil water content measurements were more often near saturation and less in the dry range (as for example in Fig. 2(a) at Gumpenstein). The θ_s parameter was therefore mostly better informed by the measurements than θ_r.

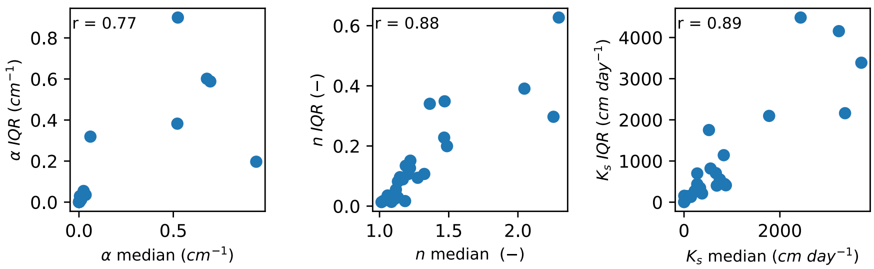

Figure 3. Correlations between median parameter estimates and 95% interquantile range (IQR) from posterior parameter distributions for α, n and K_s including 14 sites with each two soil layers. Spearman's Rho correlation coefficient (r) are given. The presented correlations for α, n and Ks were significant with p<0.01; no such relation was found for θ_s and θ_r.

Overall, SHP estimation using soil water content monitoring data from different depth levels was associated with some uncertainty. Parameter uncertainties were higher in coarse than in fine textured soils: Uncertainties in terms of the 95% interquantile range (IQR) in the posterior distributions of K_s and n were positively correlated with the percentage in sand (p=0.06); IQRs in K_s, α, and n increased significantly with the values of the median estimates (p<0.01) (Fig. 3), whereas no such relation existed for θ_s and θ_r.

The reliability of the calibration was quantified by the RMSE between median simulations and observations during calibration and validation periods, summarized for all sites in the Appendix in Table A2. Overall, the calibration fit was good, with RMSE values ranging between 0.009-0.028 cm^3 cm^{-3}. For the validation periods, the fit in terms of RMSE deteriorated especially for the locations of Lobau (RMSE calibration = 0.028 cm^3 cm^{-3}, RMSE validation = 0.054 cm^3 cm^{-3}) and Pettenbach (RMSE calibration = 0.020 cm^3 cm^{-3}, RMSE validation = 0.067 cm^3 cm^{-3}). The Lobau soil profile was under the influence of water table fluctuations where we cannot exclude that model assumptions about the lower boundary condition have been occasionally violated. At the Pettenbach lysimeter station, a crop rotation including fertilization was applied. It is possible, that this affected soil properties, which were assumed to be constant in the modeling. For example, Lu et al. (2020) showed in their review that root growth and decay can alter soil hydraulic properties; Whalley et al. (2005) found, that growing different plants had a significant effect on the porosity of the soil aggregates, and Schjønning et al. (2002) observed the development different pore systems in soils depending on crop rotation and fertilization.

Overall, the validation of the models was acceptable with RMSE values ranging between 0.014-0.067 cm^3 cm^{-3}. Scatterplots including the coefficients of determination R^2 (0.34 – 0.98) for the validation period are shown in Fig. A2 in the Appendix.

3.2 Simulated long-term water balance at the local scale

The calibrated models were used to simulate and assess different components of the water balance for all monitoring stations. In particular, we looked at long-term estimates and temporal variability in actual evapotranspiration and potential groundwater

https://doi.org/10.5194/hess-2022-261
Preprint. Discussion started: 2 August 2022

Hydrology and Earth System Sciences
Discussions

Table 2. Local long-term average water balances at 14 sites: Precipitation (P), potential Evapotranspiration (ET_p); simulated potential groundwater recharge (GWR) and actual evapotranspiration (ET_a) including 95% credible interval from propagated parameter uncertainty.

	Period	P (mm a^{-1})	ET_p(mm a^{-1})	GWR (mm a^{-1})	ET_a(mm a^{-1})	GWR/P (%)
Lauterach	1996 – 2018	1578	700	907^{+4}_{-4}	672^{+3}_{-4}	$57^{+1}_{-0}\%$
Leutasch	2008 – 2018	1235	622	665^{+9}_{-7}	521^{+7}_{-10}	$54^{+2}_{-1}\%$
Achenkirch	2017 – 2018	1533	673	1022^{+14}_{-16}	480^{+14}_{-14}	$67^{+1}_{-1}\%$
Gschlössboden	2012 – 2018	1493	552	1319^{+7}_{-9}	170^{+2}_{-6}	$88^{+0}_{-1}\%$
Sillianberger Alm	1997 – 2018	1023	707	578^{+13}_{-12}	439^{+10}_{-13}	$57^{+1}_{-1}\%$
Zettersfeld	2012 – 2018	1353	634	926^{+15}_{-10}	399^{+10}_{-15}	$68^{+1}_{-1}\%$
Elsbethen	1996 – 2018	1468	665	853^{+10}_{-6}	614^{+6}_{-10}	$58^{+1}_{-0}\%$
Gumpenstein	1996 – 2018	1100	661	641^{+8}_{-11}	448^{+11}_{-8}	$58^{+1}_{-1}\%$
Aichfeld-Murb.	1996 – 2018	813	728	244^{+3}_{-2}	557^{+2}_{-3}	$30^{+0}_{-0}\%$
Kalsdorf	1996 – 2018	852	801	229^{+23}_{-24}	623^{+19}_{-31}	$27^{+3}_{-3}\%$
Pettenbach	1996 – 2018	1031	789	459^{+18}_{-19}	558^{+20}_{-20}	$45^{+2}_{-2}\%$
Schalladorf	1996 – 2018	484	893	45^{+7}_{-7}	431^{+6}_{-7}	$9^{+1}_{-1}\%$
Lobau	1996 – 2018	570	913	44^{+8}_{-9}	520^{+9}_{-8}	$8^{+1}_{-2}\%$
Frauenkirchen	2005 – 2018	601	882	92^{+15}_{-9}	526^{+10}_{-16}	$15^{+2}_{-1}\%$

recharge, as well as the average fractions of potential groundwater recharge from precipitation. Long-term averages of input and simulated annual water balance components including propagated parameter uncertainties are given in Table 2.

Uncertainty in the estimated long-term potential annual recharge from propagated parameter uncertainty was highest in Kalsdorf (95% IQR = 47 mm) and lowest in Aichfeld-Murboden (95% IQR = 5 mm). The relative uncertainty (IQR/median) was greater at the dry sites with low absolute potential recharge estimates. It ranged between 1% (Gschlössboden, Lauterach) and 39% (Lobau). The uncertainties presented here result from parameter uncertainties from the calibration, as well as from the sensitivity of the simulated water fluxes towards the parameters (and thus also the model input data/ boundary condition during the long-term simulation periods). Some processes were not accounted for which may have affected water balances additionally: The modeling approach assumed that the groundwater table was well below the model domain at all times. At the Lobau site, however, the groundwater table is shallow, and fluctuations may have reached into the model domain. In this case, infiltrating water may have reached the water table earlier than assumed by the model. At the same time, net recharge would have been reduced if the capillary fringe extended into the root zone or even to the soil surface and transpiration and evaporation occurred directly from groundwater (Doble and Crosbie, 2017). Further, the modeling approach here neglected preferential and lateral flow processes. The ground surface at the measurement locations was even; however, it has been shown that heterogeneity and layering in the soil profiles can lead to lateral flow, even when the effective hydraulic gradient is vertical (Heilig et al., 2003; Rimon et al., 2007).

Hydrology and Earth System Sciences
Discussions

To assess the plausibility of estimated potential recharge rates we compared them to literature values where available. Tóth et al. (2016) assumed annual groundwater recharge for the western Pannonian Basin of 70 mm a^{-1}. The region includes the three southeasternmost sites here (Lobau, Frauenkirchen and Kalsdorf), where potential recharge rates in this study ranged between 44 – 229 mma^{-1}. For Wagna in southern Styria, 20 km from Kalsdorf, between 296 – 396 mm a^{-1} have been estimated in studies by Collenteur et al. (2021) and Stumpp et al. (2009). We also compared the estimates with the long-term (1961-1990) water balance averages for precipitation, potential and actual evapotranspiration on the catchment scale from the Hydrological Atlas of Austria (HAO) (BMLFUW, 2007; Dobesch, 2007; Kling et al., 2007b, a) (Fig. A3 in the Appendix). The mean annual areal actual evapotranspiration estimates of the HAO (Kling et al., 2007a) are based on water balance calculations from the period 1961 to 1990. They are comparable to our long-term estimates (R^2 = 0.78) supporting the plausibility of the here established water balances.

We further evaluated estimated recharge rates at the locations of Leutasch and Gumpenstein by comparing the available lysimeter outflow measurements to modelled median estimates. It resulted in acceptable fits of R^2 = 0.56 (for the period 2008 – 2018) and R^2 = 0.64 (for the period 2001 – 2018), respectively, and is shown in Fig. A4 in the Appendix, including uncertainties. Variability in annual seepage measurements between four Gumpenstein lysimeters was high with an average uncertainty range of 132 mm a^{-1}. This clearly exceeded the average range of predictive uncertainty related to parameter uncertainty of the modeling at this site (20 mm a^{-1}). Besides the uncertainty in the seepage measurement, the variability in the measurements could also be an indicator of spatial heterogeneities causing differences in the soil hydrology for individual lysimeters. In any case, the high variability in seepage measurements here emphasizes the need to analyze uncertainties in the estimation of soil water fluxes.

3.3 Statistical analysis of hydrologically relevant properties

The seasonal variability in groundwater recharge (quantified as coefficient of variation from standard deviation between monthly sums and annual means) ranged between 71% and 265%. This was consistently higher than the seasonality in precipitation (52 – 76%) and potential evapotranspiration (64 – 76%) indicating that potential recharge rates vary significantly more over the year than the meteorological input variables. We further analyzed the seasonality in local water balances in a PCA and correlation analysis. Figure 4 shows the biplots of the PCA, according to amount and seasonality of water balance components, the fraction of potential groundwater recharge from precipitation, and site specific properties (altitude and longitude; sand, silt, clay and organic matter percentages of the upper soil layers). PC1 and 2 alone explained 77%, PC1 – 4 together explained 93% of the variance in the data.

Two clusters were established: The five sites in the south and east of Austria (Aichfeld (9), Kalsdorf (10), Schalladorf (12), Lobau (13), Frauenkirchen (14)) show a potential recharge fraction of less than 30% of annual precipitation (as low as 8% in Lobau), a high seasonality in groundwater recharge (134 – 265%) and precipitation (67 – 76%), but a low seasonality in actual evapotranspiration (59 – 73%). The remaining nine out of 14 sites in western to central Austria with humid to wet climate show a fraction of potential groundwater recharge from precipitation of more than 40%, and a low seasonality in precipitation (52 – 68%). The seasonality in groundwater recharge at these sites was lower than in the East (71 – 124%), but seasonality in

https://doi.org/10.5194/hess-2022-261
Preprint. Discussion started: 2 August 2022

Hydrology and Earth System Sciences
Discussions

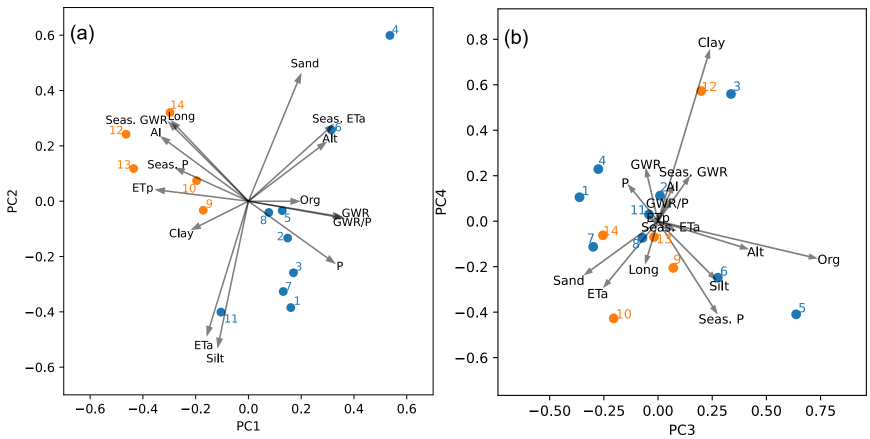

Figure 4. Principle Component Analysis biplots (a) for the first and second principle component and (b) for the third and fourth principal component. The analysis included potential annual groundwater recharge (GWR), annual precipitation (P), annual potential evapotranspiration (ET_p), annual actual evapotranspiration (ET_a), the fraction of groundwater from precipitation (GWR/P), seasonalities (Season.) in GWR, P, ET_a; longitude (Long), altitude (Alt); sand, silt, clay and organic matter (Org) percentages at the 14 sites. Clusters of monitoring sites shown in orange and blue were established with Agglomerative Clustering (Euclidean affinity and ward linkage) (Pedregosa et al., 2011).

actual evapotranspiration was higher (75 – 112%); it was most pronounced at the three sub-alpine sites (Gschlössboden (4), Sillianberger Alm (5), and Zettersfeld (6)) which were influenced by snow and where little to no actual evapotranspiration was estimated outside of the extended summer period (May – September). An obvious outlier among the monitoring sites in Fig. 4(a) was the location Gschlössboden at high altitude, with coarse soil, lowest potential and actual evapotranspiration, and the highest estimated potential recharge rates compared to other sites.

Figure 5 shows the pair-wise scatterplots, correlation coefficients and significance levels of relevant variables. Since precipitation and potential evapotranspiration were negatively correlated, we adopted the Aridity Index (ET_p/P) as predictor instead of looking at both variables separately. Seasonality in potential evapotranspiration is not shown, since no significant correlations to other variables were identified. Grain size classes of the soil textures were intercorrelated, we therefore only used the sand fraction as predictor variable.

Potential annual groundwater recharge rates were negatively correlated with aridity (lower precipitation and higher potential evapotranspiration). This was expected and was also supported by findings of (Moeck et al., 2020) on the global scale. At the Austrian sites, aridity increased and potential groundwater recharge decreased significantly with longitude, resulting in lower potential recharge rates at the eastern than at the western sites. As expected, precipitation was also correlated with altitude and so were potential recharge rates; however, less strongly and less significantly than with longitude. In the study here, slopes were not taken into consideration, as the monitoring sites were horizontally even and the modeling domain was limited to the plot scale. Regarding the larger scale (and actual recharge rates), the occurrence of steep slopes at high altitudes would be expected

https://doi.org/10.5194/hess-2022-261
Preprint. Discussion started: 2 August 2022

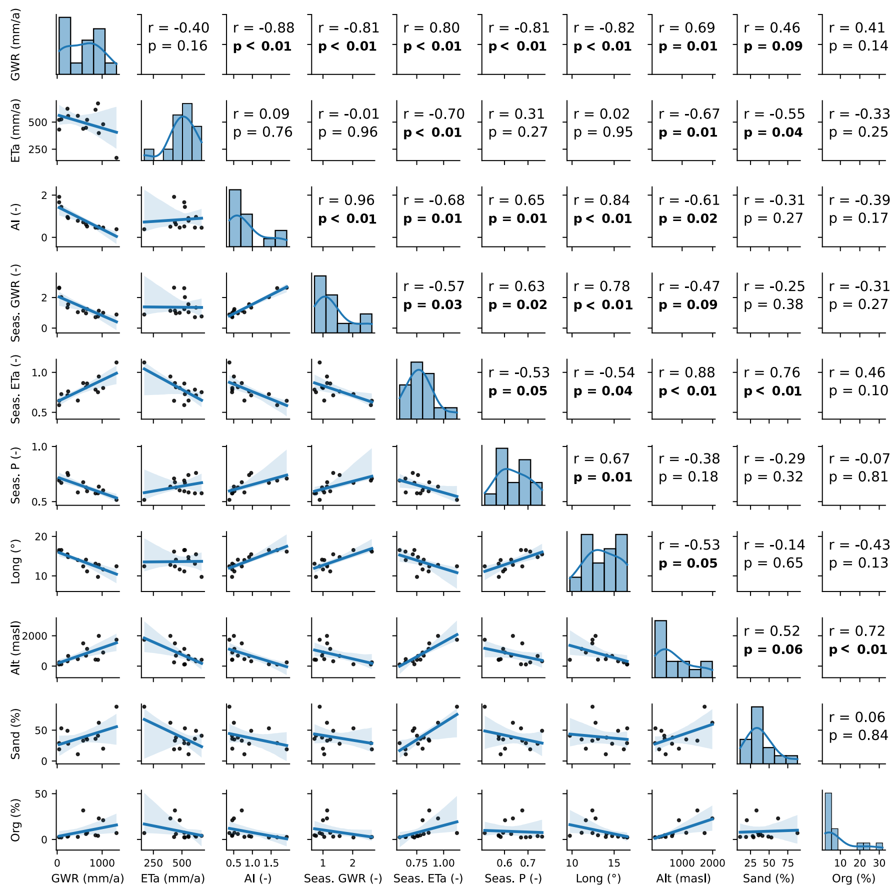

Figure 5. Correlation analysis with pair-wise scatter plots, Spearman's Rho correlation coefficient and significance levels for the variables potential annual groundwater recharge (GWR), annual actual evapotransiration (ET_a), Aridity Index (AI), Seasonalities (Seas.) in GWR, ET_a, and P; longitude (Long), altitude (Alt), percentages in sand and organic matter (Org) at 14 monitoring sites.

to result in more surface runoff or more interflow instead of recharge (Brunetti et al., 2022; Moeck et al., 2020) which could reverse the correlation of recharge rates with altitude.

The fraction of potential groundwater recharge to precipitation (GWR/P) was strongly correlated with the amount of precipitation (r = 0.91, p<0.001) which means that there is an exponential relationship between potential recharge estimates and precipitation. Similarly, Barron et al. (2012) found an exponential relationship between annual recharge and rainfall estimates at Australian sites, which they explained by the correlation of high amounts of precipitation with high rainfall intensities and long wet periods throughout the year, leading to an increased fraction of recharge from precipitation.

Higher potential recharge rates and lower actual evapotranspiration were correlated with a higher percentage in sand. Soils with greater sand fraction and less fine material have a higher hydraulic conductivity and a lower water retention capacity as they let water percolate faster below the root zone (Emerson, 1995; Wohling et al., 2012). Wang et al. (2009) observed

https://doi.org/10.5194/hess-2022-261
Preprint. Discussion started: 2 August 2022

Hydrology and Earth System Sciences
Discussions

how the fraction of recharge from precipitation increased with coarser soil texture as the more rapid deep percolation reduced evapotranspiration. In the study here, however, the relation between potential groundwater recharge and soil texture was weaker compared to climatic factors, i.e. precipitation and potential evapotranspiration. This corresponded to findings of the global scale analysis by Moeck et al. (2020).

Seasonality in potential groundwater recharge was most strongly correlated with the Aridity Index (ET_p/P). Sites in the east, with more pronounced aridity and low potential recharge rates, were associated with a high seasonality with extended periods of zero recharge. Estimated potential groundwater recharge there was concentrated on the winter half-year. High rates in potential groundwater recharge were associated with sites where recharge occurred throughout the year and were thus correlated with a low seasonality in recharge. Soil texture did not correlate with seasonality in estimated potential groundwater recharge. In this study, we assumed the same lower boundary for all profiles to ensure comparability of the sites, where additional data from below 1.5 m were not available. However, the depth of the water table, and thus the thickness of the unsaturated zone, in addition to structural features causing lateral flow, determine quantity and timing of water actually reaching the aquifer. With greater thickness of the unsaturated zone, the influence of soil water retention characteristics on magnitude and temporal variability of actual groundwater recharge rates might increase (Burri et al., 2019; Cao et al., 2016; Moeck et al., 2020). In future, data from the deeper unsaturated zone (>1.5 m) would be helpful to further improve the quantification of recharge.

4 Conclusions

In this study, we made use of volumetric soil water content measurements from multiple depth levels at 14 locations in Austria to inversely estimate effective soil hydraulic parameters (SHPs) using the physically based HYDRUS-1D model, and we quantified parameter uncertainties in a Bayesian probabilistic framework based on multimodal Nested Sampling. We used the calibrated models for the long-term simulation of soil water fluxes and associated uncertainties. Finally, we compared potential recharge rates and actual evapotranspiration at the 14 Austrian locations to identify the influencing factors on amount and temporal variability of local water balances.

SHPs were successfully established resulted in good fits to the measured soil water content. The parameter estimation based on soil water content measurements was partly subject to considerable uncertainties; especially in the residual water content and soil hydraulic conductivity parameters, whereas uncertainties in the estimation of saturated water content parameters and shape parameters n of the soil water retention curves were low. Higher uncertainties in shape parameters and the saturated hydraulic conductivity parameter were linked with coarser soil textures. The absolute uncertainty in potential groundwater recharge derived from SHP uncertainty ranged between 5-47 mm a^{-1}; the relative uncertainty (IQR/median) was as low as 1% at sites with high absolute potential recharge rates in a wet climate, and as high as 39% with low absolute potential recharge rates in a dry climate.

Estimated potential groundwater recharge rates at the Austrian soil water monitoring sites were influenced by the East-West gradient in altitude and climatic conditions: The dry continental climate at the eastern locations was associated with low fractions of potential groundwater recharge from precipitation, and high seasonality in potential recharge rates. In contrast,

Hydrology and Earth System Sciences
Open Access
Discussions

the wet and snow influenced climate at western and central Austrian sites came with high potential recharge rates and lower temporal variability in recharge than in the East, but with a higher seasonality in actual evapotranspiration. Sandy soil textures were associated with higher potential recharge rates and lower actual evapotranspiration. However, precipitation and potential evapotranspiration were more influential variables than soil properties on estimated potential recharge rates and their temporal variability.

Overall, the use of a Nested Sampling based Bayesian approach proved to be an efficient method to inversely estimate SHPs and soil water fluxes, and to quantify associated uncertainties from soil water monitoring data. The calibrated models can be used to estimate future groundwater recharge rates under climate change and to illuminate model uncertainties resulting from SHP uncertainties and a range of climate scenarios.

Author contributions. MS, GB and CS designed the study, MS and GB performed the model simulations and contributed Python code for the analysis and data visualization. MS conducted the statistical analysis. GF curated and provided the original data. MS wrote the initial draft, CS, GB and GF reviewed and edited the manuscript. All authors revised the paper and agreed on its contents.

Competing interests. The authors declare that they have no conflict of interest.

Acknowledgements. This work was carried out in the framework of the RechAUT project and supported by the Austrian Academy of Sciences (ÖAW), Vienna, Austria. Meteorological data was provided by the Central Institution for Meteorology and Geodynamics (ZAMG), Vienna, Austria. Soil texture data for the site of Gschlössboden was provided by the Hydrography and Hydrology Division of the Tyrolean Government.

https://doi.org/10.5194/hess-2022-261
Preprint. Discussion started: 2 August 2022

Hydrology and Earth System Sciences
Open Access
EGU
Discussions

Appendix A

Table A1. Site properties, particle size distribution of the upper soil layer (ÖNORM L 1050), and selected measurement depths for calibration and validation periods.

	Altitude (m.a.s.l.)	Longitude (°)	Latitude (°)	Sand % $0.063-2.0$ mm	Silt % $0.002-0.063$ mm	Clay % <0.002 mm	Probe dephts ($-$cm)
Lauterach	415	9.74	47.48	41	45	14	10, 30, 60, 120
Leutasch	1135	11.14	47.37	35	51	14	10, 50, 80
Achenkirch	895	11.64	47.58	20	48	32	5, 25, 50
Gschlössboden	1737	12.43	47.12	88	12	0	10, 20, 30
Sillianberger Alm	1500	12.41	46.76	33	63	4	10, 20, 30, 50
Zettersfeld	1990	12.79	46.87	56	42	2	20, 40, 60
Elsbethen	428	13.08	47.76	36	59	5	10, 30, 60, 90, 150
Gumpenstein	690	14.10	47.50	38	53	9	20, 40
Aichfeld-Murb.	669	14.76	47.21	28	56	16	10, 30, 90, 150
Kalsdorf	320	15.47	46.95	49	42	9	10, 30, 60, 130, 150
Pettenbach	466	14.01	47.98	11	75	14	10, 35, 60
Schalladorf	238	16.14	48.64	17	43	40	35, 60, 90, 120, 150
Lobau	150	16.53	48.21	29	57	14	5, 10, 35, 150
Frauenkirchen	124	16.90	47.85	53	33	14	10, 40, 80, 110, 145

https://doi.org/10.5194/hess-2022-261
Preprint. Discussion started: 2 August 2022

Hydrology and Earth System Sciences
Open Access
EGU
Discussions

Table A2. Calibration and validation periods, and goodness of fit (root mean squared error RMSE) between median prediction and measurements.

	Calibration	Validation	Calib. RMSE $(\mathrm{cm^3\ cm^{-3}})$	Valid. RMSE $(\mathrm{cm^3\ cm^{-3}})$
Lauterach	01.03. – 31.10.2015	01.01.2016 – 31.12.2016	0.025	0.028
Leutasch	01.03. – 31.10.2014	01.03.2017 – 31.10.2017	0.018	0.021
Achenkirch	01.05. – 31.10.2018	01.01.2017 – 31.12.2017	0.023	0.037
Gschlössboden*	01.04. – 30.09.2018	01.01.2018 – 31.12.2018	0.017	0.019
Sillianberger Alm*	01.03. – 31.10.2018	01.01.2018 – 31.12.2018	0.026	0.020
Zettersfeld	01.04. – 30.09.2017	01.01.2014 – 31.12.2015	0.022	0.020
Elsbethen	01.03. – 31.10.2015	01.01.2012 – 31.12.2012	0.018	0.015
Gumpenstein	15.04. – 15.10.2012	01.03.2011 – 31.12.2011	0.011	0.014
Aichfeld-Murb.	15.04. – 15.10.2016	15.08.2017 – 31.12.2018	0.015	0.021
Kalsdorf	01.03. – 31.10.2007	01.01.2008 – 31.12.2008	0.021	0.037
Pettenbach**	23.04. – 14.10.2014	24.04.2013 – 24.09.2013	0.020	0.067
Schalladorf	01.03. – 31.10.2010	01.03.2013 – 31.10.2014	0.009	0.028
Lobau	01.03. – 31.10.2012	01.01.2000 – 31.12.2000	0.028	0.054
Frauenkirchen	01.03. – 31.10.2015	01.01.2012 – 31.12.2014	0.021	0.036

* No validation data available outside the calibration year, instead the RMSE for the entire year (2018) was calculated.

** Pettenbach calibration period during maize cultivation, validation period during soy bean cultivation. Root parameters were adjusted and potential evapotranspiration estimation was estimated with corresponding crop coefficients (Allen et al., 1998).

https://doi.org/10.5194/hess-2022-261
Preprint. Discussion started: 2 August 2022

Hydrology and Earth System Sciences
Discussions

Table A3. Soil layers in HYDRUS-1D and prior parameter ranges of the Bayesian analysis.

Site		Depth (cm)	$\theta_r\ (\mathrm{cm^3\ cm^{-3}})$	$\theta_s\ (\mathrm{cm^3\ cm^{-3}})$	$\alpha\ (\mathrm{cm^{-1}})$	$n(-)$	$K_s\ (\mathrm{cm\ d^{-1}})$
Lauterach	L1	0 – 24	0.00 – 0.20	0.30 – 0.50	0.0001 – 0.1000	1.01 – 2.00	1 – 200
	L2	25 – 150	0.00 – 0.20	0.30 – 0.50	0.0001 – 0.1000	1.01 – 2.00	1 – 200
Leutasch	L1	0 – 24	0.00 – 0.10	0.25 – 0.50	0.0001 – 0.5000	1.01 – 2.70	1 – 1000
	L2	25 – 150	0.00 – 0.10	0.15 – 0.40	0.0001 – 0.5000	1.01 – 3.50	1 – 1000
Achenkirch	L1	0 – 15	0.00 – 0.25	0.40 – 0.60	0.0001 – 0.5000	1.01 – 2.70	1 – 1000
	L2	16 – 150	0.00 – 0.08	0.10 – 0.20	0.0001 – 1.0000	1.01 – 3.50	10 – 10000
Gschlössboden	L1	0 – 22	0.00 – 0.05	0.20 – 0.35	0.0001 – 1.0000	1.01 – 2.70	10 – 10000
	L2	23 – 150	0.00 – 0.05	0.20 – 0.35	0.0001 – 1.0000	1.01 – 3.50	10 – 10000
Sillianberger Alm	L1	0 – 24	0.00 – 0.20	0.30 – 0.60	0.0001 – 0.2000	1.01 – 2.00	1 – 5000
	L2	25 – 150	0.00 – 0.20	0.30 – 0.60	0.0001 – 0.2000	1.01 – 2.00	1 – 5000
Zettersfeld	L1	0 – 49	0.00 – 0.25	0.30 – 0.60	0.0001 – 1.0000	1.01 – 2.70	1 – 5000
	L2	50 – 150	0.00 – 0.08	0.10 – 0.40	0.0001 – 1.0000	1.01 – 3.50	1 – 5000
Elsbethen	L1	0 – 24	0.00 – 0.20	0.30 – 0.50	0.0001 – 0.1000	1.01 – 2.00	1 – 200
	L2	25 – 150	0.00 – 0.20	0.30 – 0.50	0.0001 – 0.1000	1.01 – 2.00	1 – 200
Gumpenstein	L1	0 – 24	0.00 – 0.20	0.25 – 0.60	0.0001 – 0.5000	1.01 – 2.70	0.1 – 500
	L2	25 – 150	0.00 – 0.20	0.25 – 0.60	0.0001 – 0.5000	1.01 – 2.70	0.1 – 500
Aichfeld-Murboden	L1	0 – 74	0.00 – 0.25	0.30 – 0.60	0.0001 – 0.5000	1.01 – 2.70	1 – 1000
	L2	75 – 150	0.00 – 0.15	0.17 – 0.40	0.0001 – 1.0000	1.01 – 2.70	1 – 1000
Kalsdorf	L1	0 – 24	0.00 – 0.10	0.30 – 0.60	0.0001 – 0.2000	1.01 – 2.00	1 – 1000
	L2	25 – 150	0.00 – 0.10	0.30 – 0.60	0.0001 – 0.2000	1.01 – 2.00	1 – 1000
Pettenbach	L1	0 – 24	0.00 – 0.25	0.30 – 0.60	0.0001 – 0.5000	1.01 – 2.70	0.1 – 500
	L2	25 – 150	0.00 – 0.25	0.30 – 0.60	0.0001 – 1.0000	1.01 – 2.70	0.1 – 500
Schalladorf	L1	0 – 44	0.00 – 0.20	0.40 – 0.60	0.0001 – 0.1000	1.01 – 2.00	1 – 50
	L2	45 – 150	0.00 – 0.20	0.30 – 0.50	0.0001 – 0.1000	1.01 – 2.00	1 – 50
Lobau	L1	0 – 100	0.00 – 0.15	0.35 – 0.75	0.0001 – 1.0000	1.01 – 2.70	1 – 1000
	L2	101 – 150	0.00 – 0.25	0.35 – 0.60	0.0001 – 1.0000	1.01 – 2.70	1 – 1000
Frauenkirchen	L1	0 – 24	0.00 – 0.20	0.30 – 0.60	0.0001 – 0.2000	1.01 – 2.00	1 – 500
	L2	25 – 150	0.00 – 0.20	0.30 – 0.60	0.0001 – 0.2000	1.01 – 2.00	1 – 500

Hydrology and Earth System Sciences
Open Access
Discussions

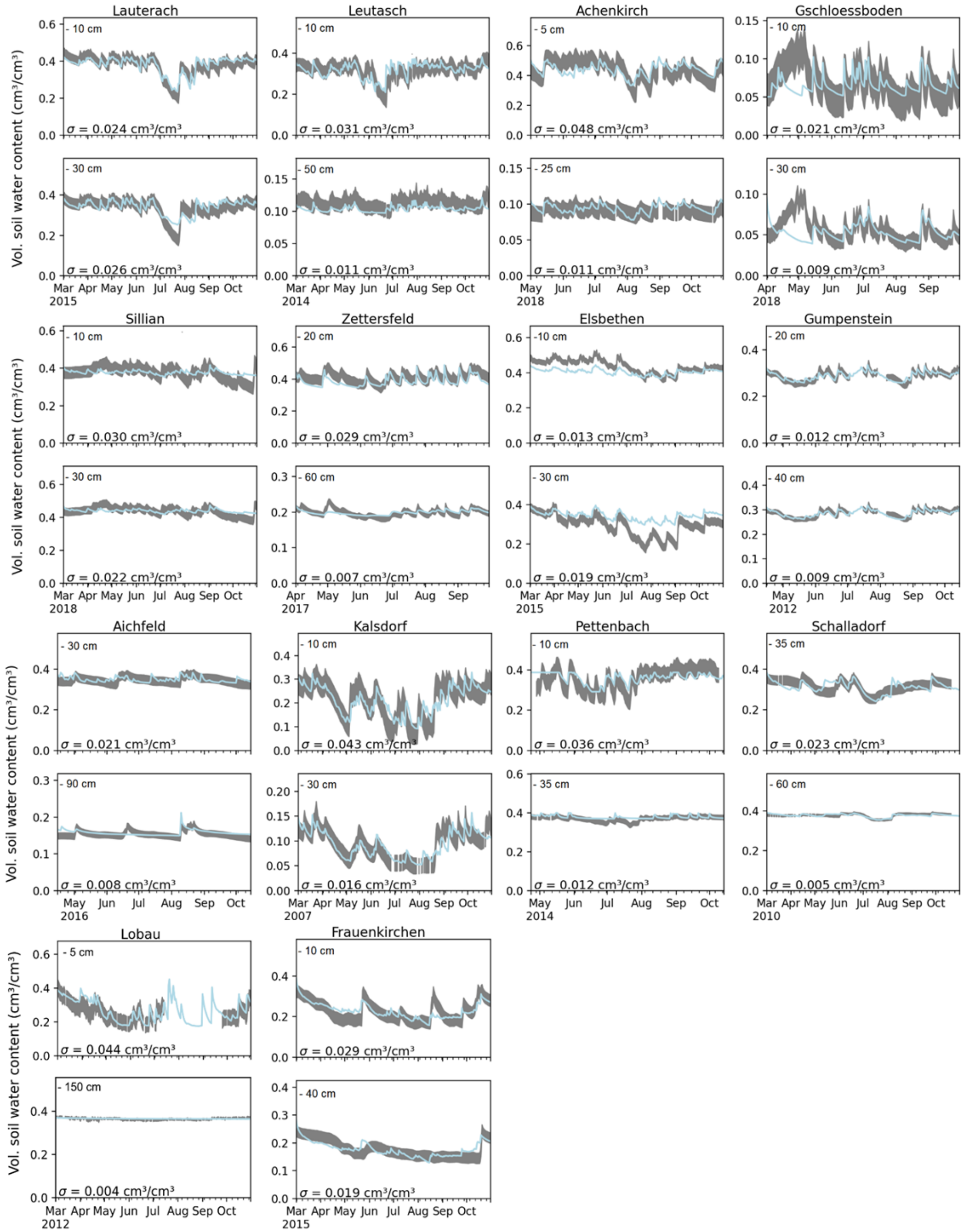

Figure A1. Calibration with soil water content measurements at all 14 sites: The grey bands show the measurement including the area of the calibrated measurement error σ, the blue lines show the prediction with median parameter estimates for each one measurement depth in upper and lower soil layer.

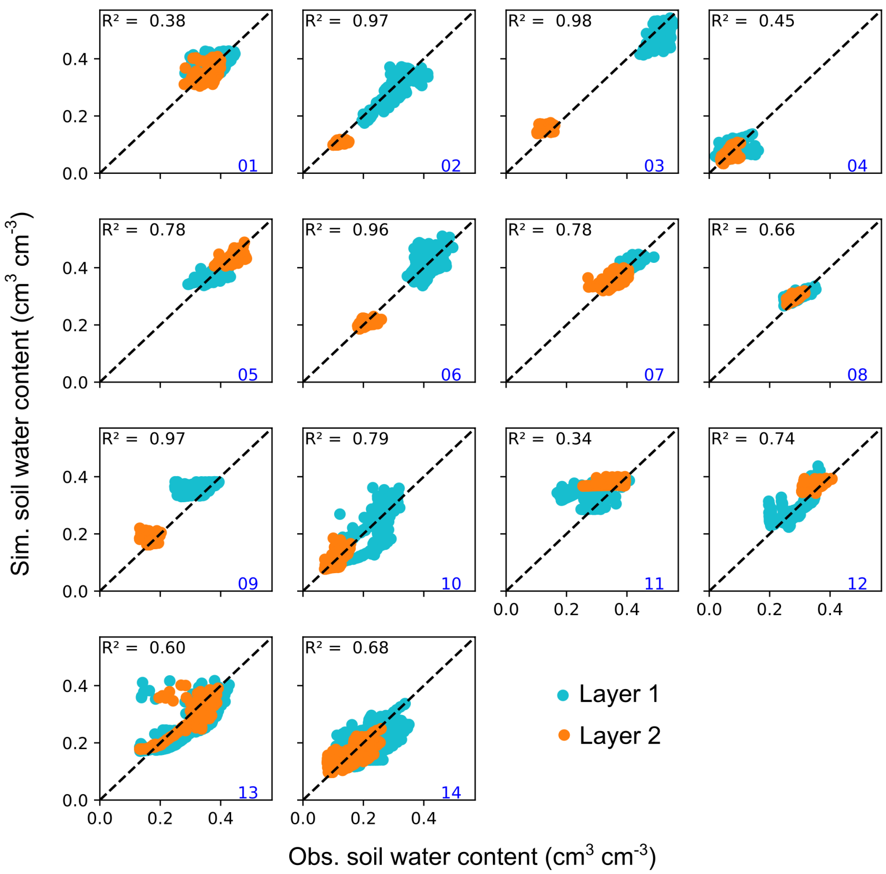

Figure A2. Model validation showing the coefficient of determination (R^2) and scatterplots of simulated and observed soil water content from upper and lower soil layer (layer 1 and 2, respectively) for the 14 sites: (01) Lauterach, (02) Leutasch, (03) Achenkirch, (04) Gschlössboden, (05) Sillianberger Alm, (06) Zettersfeld, (07) Elsbethen, (08) Gumpenstein, (09) Aichfeld-Murboden, (10) Kalsdorf, (11) Pettenbach, (12) Schalladorf, (13) Lobau, (14) Frauenkirchen. Validation periods are given in Table A2.

https://doi.org/10.5194/hess-2022-261
Preprint. Discussion started: 2 August 2022

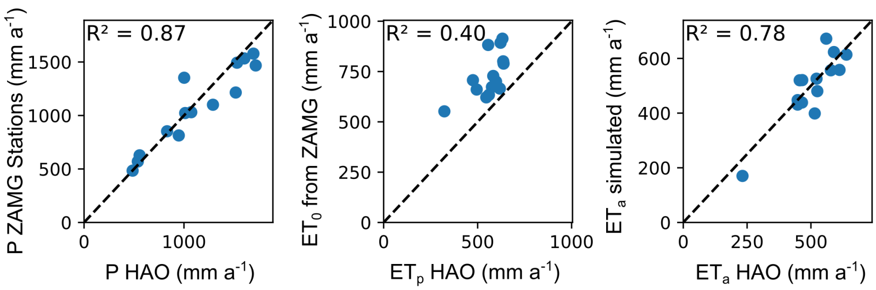

Figure A3. Scatterplots comparing the long-term averages of precipitation (P), potential and actual evapotranspiration (ET_p and ET_a) from the digital Hydrological Atlas of Austria (HAO) (BMLFUW, 2007) with the corresponding rates of simulations in this study. Potential evapotranspiration in the HAO was calculated by Dobesch (2007) using the FAO approach described by Doorenbos and Pruitt (1977) resulting in lower values than those of this study which were calculated for a grass reference according to Allen et al. (1998).

https://doi.org/10.5194/hess-2022-261
Preprint. Discussion started: 2 August 2022

Hydrology and Earth System Sciences
Discussions

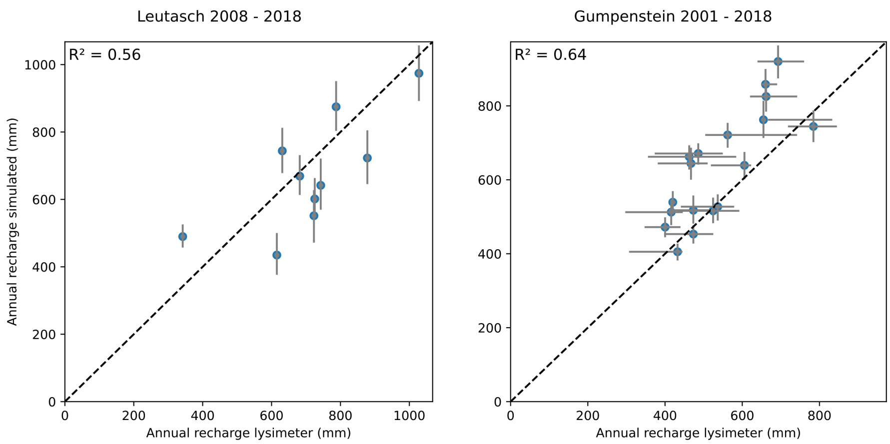

Figure A4. Model validation using lysimeter data from Leutasch and Gumpenstein. Scatterplots and coefficients of determination (R^2) are shown for simulated and observed annual seepage flow. Grey errorbars depict the 95% credible interval from propagated parameter uncertainty. Leutasch seepage measurements are obtained from a single lysimeter; for Gumpenstein, the 95% uncertainty interval in lysimeter measurements was calculated from a cluster of four lysimeters.

References

Allen, R. G., Pereira, L. S., Raes, D., Smith, M., and Others: FAO Irrigation and drainage paper No. 56, Rome: Food and Agriculture Organization of the United Nations, 56, e156, 1998.

Barkle, G., Wöhling, T., Stenger, R., Mertens, J., Moorhead, B., Wall, A., and Clague, J.: Automated Equilibrium Tension Lysimeters for Measuring Water Fluxes through a Layered, Volcanic Vadose Profile in New Zealand, Vadose Zone Journal, 10, 747–759, https://doi.org/10.2136/vzj2010.0091, 2011.

Baroni, G., Facchi, A., Gandolfi, C., Ortuani, B., Horeschi, D., and Van Dam, J. C.: Uncertainty in the determination of soil hydraulic parameters and its influence on the performance of two hydrological models of different complexity, Hydrology and Earth System Sciences, 14, 251–270, https://doi.org/10.5194/hess-14-251-2010, 2010.

Barron, O. V., Crosbie, R. S., Dawes, W. R., Charles, S. P., Pickett, T., and Donn, M. J.: Climatic controls on diffuse groundwater recharge across Australia, Hydrology and Earth System Sciences, 16, 4557–4570, https://doi.org/10.5194/hess-16-4557-2012, 2012.

Berthelin, R., Rinderer, M., Andreo, B., Baker, A., Kilian, D., Leonhardt, G., Lotz, A., Lichtenwoehrer, K., Mudarra, M., Y. Padilla, I., Pantoja Agreda, F., Rosolem, R., Vale, A., and Hartmann, A.: A soil moisture monitoring network to characterize karstic recharge and evapotranspiration at five representative sites across the globe, Geoscientific Instrumentation, Methods and Data Systems, 9, 11–23, https://doi.org/10.5194/gi-9-11-2020, 2020.

Beven, K.: A manifesto for the equifinality thesis, Journal of Hydrology, 320, 18–36, https://doi.org/10.1016/j.jhydrol.2005.07.007, 2006.

BFW: Österreichische Bodenkartierung, https://bodenkarte.at/, 2016.

BMLFUW: Hydrologischer Atlas Österreichs, 2007.

Boumaiza, L., Chesnaux, R., Walter, J., and Stumpp, C.: Assessing groundwater recharge and transpiration in a humid northern region dominated by snowmelt using vadose-zone depth profiles, Hydrogeology Journal, 28, 2315–2329, https://doi.org/10.1007/s10040-020-02204-z, 2020.

Bresciani, E., Cranswick, R. H., Banks, E. W., Batlle-Aguilar, J., Cook, P. G., and Batelaan, O.: Using hydraulic head, chloride and electrical conductivity data to distinguish between mountain-front and mountain-block recharge to basin aquifers, Hydrology and Earth System Sciences, 22, 1629–1648, https://doi.org/10.5194/hess-22-1629-2018, 2018.

Brunetti, G., Šimůnek, J., Bogena, H., Baatz, R., Huisman, J. A., Dahlke, H., and Vereecken, H.: On the Information Content of Cosmic-Ray Neutron Data in the Inverse Estimation of Soil Hydraulic Properties, Vadose Zone Journal, 18, 1–24, https://doi.org/10.2136/vzj2018.06.0123, 2019.

Brunetti, G., Papagrigoriou, I. A., and Stumpp, C.: Disentangling model complexity in green roof hydrological analysis: A Bayesian perspective, Water Research, 182, https://doi.org/10.1016/j.watres.2020.115973, 2020a.

Brunetti, G., Šimůnek, J., Glöckler, D., and Stumpp, C.: Handling model complexity with parsimony: Numerical analysis of the nitrogen turnover in a controlled aquifer model setup, Journal of Hydrology, 584, https://doi.org/10.1016/j.jhydrol.2020.124681, 2020b.

Brunetti, G., Schübl, M., Santner, K., and Stumpp, C.: Sensitivitätsanalyse zu Infiltrationsprozessen in Böden, Österreichische Wasser- und Abfallwirtschaft, 74, 179–186, https://doi.org/10.1007/s00506-022-00839-8, 2022.

Buchner, J.: A statistical test for Nested Sampling algorithms, Statistics and Computing, 26, 383–392, https://doi.org/10.1007/s11222-014-9512-y, 2016.

Burri, N. M., Weatherl, R., Moeck, C., and Schirmer, M.: A review of threats to groundwater quality in the anthropocene, Science of the Total Environment, 684, 136–154, https://doi.org/10.1016/j.scitotenv.2019.05.236, 2019.

Cao, G., Scanlon, B. R., Han, D., and Zheng, C.: Impacts of thickening unsaturated zone on groundwater recharge in the North China Plain, Journal of Hydrology, 537, 260–270, https://doi.org/10.1016/j.jhydrol.2016.03.049, 2016.

Chesnaux, R. and Stumpp, C.: Advantages and challenges of using soil water isotopes to assess groundwater recharge dominated by snowmelt at a field study located in Canada, Hydrological Sciences Journal, 63, 679–695, https://doi.org/10.1080/02626667.2018.1442577, 2018.

Collenteur, R. A., Bakker, M., Klammler, G., and Birk, S.: Estimation of groundwater recharge from groundwater levels using non-linear transfer function noise models and comparison to lysimeter data, Hydrology and Earth System Sciences, 25, 2931–2949, https://doi.org/10.5194/hess-25-2931-2021, 2021.

Dettmann, U., Bechtold, M., Frahm, E., and Tiemeyer, B.: On the applicability of unimodal and bimodal van Genuchten-Mualem based models to peat and other organic soils under evaporation conditions, Journal of Hydrology, 515, 103–115, https://doi.org/10.1016/j.jhydrol.2014.04.047, 2014.

Dobesch, H.: Hydrological Atlas of Austria - Mean annual potential evapotranspiration (3.2), Lebensministerium (BMLFUW)(ed.). Vienna, 2007.

Doble, R. C. and Crosbie, R. S.: Revue: Méthodes courantes et émergentes pour la modélisation de la recharge à l'échelle du bassin versant et de l'évapotranspiration d'eaux souterraines peu profondes, Hydrogeology Journal, 25, 3–23, https://doi.org/10.1007/s10040-016-1470-3, 2017.

Döll, P. and Fiedler, K.: Global-scale modeling of groundwater recharge, Hydrology and Earth System Sciences, 12, 863–885, https://doi.org/10.5194/hess-12-863-2008, 2008.

Doorenbos, J. and Pruitt, W. O.: Crop evapotranspiration, FAO irrigation and drainage Paper, 24, 194, 1977.

Durner, W., Jansen, U., and Iden, S. C.: Effective hydraulic properties of layered soils at the lysimeter scale determined by inverse modelling, European Journal of Soil Science, 59, 114–124, https://doi.org/10.1111/j.1365-2389.2007.00972.x, 2008.

Dyck, M. and Kachanoski, R.: Spatial Scale-Dependence of Preferred Flow Domains during Infiltration in a Layered Field Soil, Vadose Zone Journal, 9, 385–396, https://doi.org/10.2136/vzj2009.0093, 2010.

Elsheikh, A. H., Wheeler, M. F., and Hoteit, I.: Nested sampling algorithm for subsurface flow model selection, uncertainty quantification, and nonlinear calibration, Water Resources Research, 49, 8383–8399, https://doi.org/10.1002/2012WR013406, 2013.

Emerson, W. W.: Water retention, organic c and soil texture, Australian Journal of Soil Research, 33, 241–251, https://doi.org/10.1071/SR9950241, 1995.

Feddes, R. A., Kowalik, P. J., Zaradny, H., Taylor, S. A., Ashcroft, G. L., Others, Vrugt, J. A., Diks, C. G., Gupta, H. V., Bouten, W., and Verstraten, J. M.: Physical edaphology. The physics of irrigated and nonirrigated soils., Monogr. PUDOC, Wageningen, 41, 1–17, https://doi.org/10.1029/2004WR003059, 1978.

Feroz, F. and Hobson, M. P.: Multimodal nested sampling: An efficient and robust alternative to Markov Chain Monte Carlo methods for astronomical data analyses, Monthly Notices of the Royal Astronomical Society, 384, 449–463, https://doi.org/10.1111/j.1365-2966.2007.12353.x, 2008.

Feroz, F., Hobson, M. P., and Bridges, M.: MultiNest: An efficient and robust Bayesian inference tool for cosmology and particle physics, Monthly Notices of the Royal Astronomical Society, 398, 1601–1614, https://doi.org/10.1111/j.1365-2966.2009.14548.x, 2009.

Feroz, F., Hobson, M. P., Cameron, E., and Pettitt, A. N.: Importance Nested Sampling and the MultiNest Algorithm, The Open Journal of Astrophysics, 2, https://doi.org/10.21105/astro.1306.2144, 2019.

Finsterle, S.: Practical notes on local data-worth analysis, Water Resources Research, 51, 9904–9924, https://doi.org/10.1002/2015WR017445, 2015.

Fuentes, C., Haverkamp, R., and Parlange, J. Y.: Parameter constraints on closed-form soilwater relationships, Journal of Hydrology, 134, 117–142, https://doi.org/10.1016/0022-1694(92)90032-Q, 1992.

Groh, J., Vanderborght, J., Pütz, T., and Vereecken, H.: How to Control the Lysimeter Bottom Boundary to Investigate the Effect of Climate Change on Soil Processes?, Vadose Zone Journal, 15, vzj2015.08.0113, https://doi.org/10.2136/vzj2015.08.0113, 2016.

Groh, J., Stumpp, C., Lücke, A., Pütz, T., Vanderborght, J., and Vereecken, H.: Inverse Estimation of Soil Hydraulic and Transport Parameters of Layered Soils from Water Stable Isotope and Lysimeter Data, Vadose Zone Journal, 17, 170 168, https://doi.org/10.2136/vzj2017.09.0168, 2018.

Hartmann, A., Goldscheider, N., Wagener, T., Lange, J., and Weiler, M.: Karst water resources in a changing world: Review of hydrological modeling approaches, Reviews of Geophysics, 52, 218–242, https://doi.org/10.1002/2013RG000443, 2014.

Hartmann, A., Gleeson, T., Wada, Y., and Wagener, T.: Enhanced groundwater recharge rates and altered recharge sensitivity to climate variability through subsurface heterogeneity, Proceedings of the National Academy of Sciences of the United States of America, 114, 2842–2847, https://doi.org/10.1073/pnas.1614941114, 2017.

Healy, R. W. and Cook, P. G.: Using groundwater levels to estimate recharge, Hydrogeology Journal, 10, 91–109, https://doi.org/10.1007/s10040-001-0178-0, 2002.

Heilig, A., Steenhuis, T. S., Walter, M. T., and Herbert, S. J.: Funneled flow mechanisms in layered soil: Field investigations, Journal of Hydrology, 279, 210–223, https://doi.org/10.1016/S0022-1694(03)00179-3, 2003.

Heppner, C. S., Nimmo, J. R., Folmar, G. J., Gburek, W. J., and Risser, D. W.: Multiple-methods investigation of recharge at a humid-region fractured rock site, Pennsylvania, USA, Hydrogeology Journal, 15, 915–927, https://doi.org/10.1007/s10040-006-0149-6, 2007.

Kaminsky, E., Plan, L., Wagner, T., Funk, B., and Oberender, P.: Flow dynamics in a vadose shaft – a case study from the hochschwab karst massif (Northern calcareous alps, austria), International Journal of Speleology, 50, 157–172, https://doi.org/10.5038/1827-806X.50.2.2375, 2021.

Keese, K. E., Scanlon, B. R., and Reedy, R. C.: Assessing controls on diffuse groundwater recharge using unsaturated flow modeling, Water Resources Research, 41, 1–12, https://doi.org/10.1029/2004WR003841, 2005.

Kling, H., Nachtnebel, H. P., and Fürst, J.: Hydrological Atlas of Austria - Mean annual areal actual evapotranspiration (3.3), Lebensministerium (BMLFUW)(ed.). Vienna, 2007a.

Kling, H., Nachtnebel, H. P., and Fürst, J.: Hydrological Atlas of Austria - Mean annual areal precipitation (2.3), Lebensministerium (BMLFUW)(ed.). Vienna, 2007b.

Koeniger, P., Gaj, M., Beyer, M., and Himmelsbach, T.: Review on soil water isotope-based groundwater recharge estimations, Hydrological Processes, 30, 2817–2834, https://doi.org/10.1002/hyp.10775, 2016.

Lambot, S., Javaux, M., Hupet, F., and Vanclooster, M.: A global multilevel coordinate search procedure for estimating the unsaturated soil hydraulic properties, Water Resources Research, 38, 6–1–6–15, https://doi.org/10.1029/2001wr001224, 2002.

Land OÖ: Forschungsprojekt Lysimeter, Technischer Endbericht 2013, Tech. rep., Amt der Oö. Landesregierung, Abteilung Grund- und Trinkwasserwirtschaft, Linz, 2013.

Land OÖ: Forschungsprojekt Lysimeter, Technischer Endbericht 2014, Tech. rep., Amt der Oö. Landesregierung, Abteilung Grund- und Trinkwasserwirtschaft, Linz., 2014.

Lu, J., Zhang, Q., Werner, A. D., Li, Y., Jiang, S., and Tan, Z.: Root-induced changes of soil hydraulic properties – A review, Journal of Hydrology, 589, https://doi.org/10.1016/j.jhydrol.2020.125203, 2020.

Minasny, B. and Field, D. J.: Estimating soil hydraulic properties and their uncertainty: The use of stochastic simulation in the inverse modelling of the evaporation method, Geoderma, 126, 277–290, https://doi.org/10.1016/j.geoderma.2004.09.015, 2005.

Mishra, S., Parker, J. C., and Singhal, N.: Estimation of soil hydraulic properties and their uncertainty from particle size distribution data, Journal of Hydrology, 108, 1–18, https://doi.org/10.1016/0022-1694(89)90275-8, 1989.

Moeck, C., von Freyberg, J., and Schirmer, M.: Groundwater recharge predictions in contrasted climate: The effect of model complexity and calibration period on recharge rates, Environmental Modelling and Software, 103, 74–89, https://doi.org/10.1016/j.envsoft.2018.02.005, 2018.

Moeck, C., Grech-Cumbo, N., Podgorski, J., Bretzler, A., Gurdak, J. J., Berg, M., and Schirmer, M.: A global-scale dataset of direct natural groundwater recharge rates: A review of variables, processes and relationships, Science of the Total Environment, 717, https://doi.org/10.1016/j.scitotenv.2020.137042, 2020.

Mualem, Y.: A new model for predicting the hydraulic conductivity of unsaturated porous media, Water Resources Research, 12, 513–522, https://doi.org/10.1029/WR012i003p00513, 1976.

Mukherjee, P., Parkinson, D., and Liddle, A. R.: A Nested Sampling Algorithm for Cosmological Model Selection, The Astrophysical Journal, 638, L51–L54, https://doi.org/10.1086/501068, 2006.

Neukum, C. and Azzam, R.: Impact of climate change on groundwater recharge in a small catchment in the Black Forest, Germany, Hydrogeology Journal, 20, 547–560, https://doi.org/10.1007/s10040-011-0827-x, 2012.

Neukum, C., Hötzl, H., and Himmelsbach, T.: Validation of vulnerability mapping methods by field investigations and numerical modelling, Hydrogeology Journal, 16, 641–658, https://doi.org/10.1007/s10040-007-0249-y, 2008.

Nolan, B. T., Healy, R. W., Taber, P. E., Perkins, K., Hitt, K. J., and Wolock, D. M.: Factors influencing ground-water recharge in the eastern United States, Journal of Hydrology, 332, 187–205, https://doi.org/10.1016/j.jhydrol.2006.06.029, 2007.

Nolz, R., Cepuder, P., and Eitzinger, J.: Comparison of lysimeter based and calculated ASCE reference evapotranspiration in a subhumid climate, Theoretical and Applied Climatology, 124, 315–324, https://doi.org/10.1007/s00704-015-1417-y, 2016.

ÖNORM L 1050, .: ÖNORM L 1050, 2004: Boden als Pflanzenstandort–Begriffe und Untersuchungsverfahren.

Pedregosa, F., Varoquaux, G., Gramfort, A., Michel, V., Thirion, B., Grisel, O., Blondel, M., Prettenhofer, P., Weiss, R., Dubourg, V., Vanderplas, J., Passos, A., Cournapeau, D., Brucher, M., Perrot, M., and Duchesnay, E.: Scikit-learn: Machine Learning in Python, Journal of Machine Learning Research, 12, 2825–2830, 2011.

Pütz, T., Fank, J., and Flury, M.: Lysimeters in Vadose Zone Research, Vadose Zone Journal, 17, 180 035, https://doi.org/10.2136/vzj2018.02.0035, 2018.

QGIS Development Team: QGIS Geographic Information System, QGIS Association, https://www.qgis.org, 2022.

Rimon, Y., Dahan, O., Nativ, R., and Geyer, S.: Water percolation through the deep vadose zone and groundwater recharge: Preliminary results based on a new vadose zone monitoring system, Water Resources Research, 43, https://doi.org/10.1029/2006WR004855, 2007.

Scanlon, B. R., Healy, R. W., and Cook, P. G.: Choosing appropriate techniques for quantifying groundwater recharge, Hydrogeology Journal, 10, 18–39, https://doi.org/10.1007/s10040-001-0176-2, 2002.

Schaap, M. G. and Leij, F. J.: Using neural networks to predict soil water retention and soil hydraulic conductivity, Soil and Tillage Research, 47, 37–42, https://doi.org/10.1016/S0167-1987(98)00070-1, 1998.

Scharnagl, B., Vrugt, J. A., Vereecken, H., and Herbst, M.: Inverse modelling of in situ soil water dynamics: Investigating the effect of different prior distributions of the soil hydraulic parameters, Hydrology and Earth System Sciences, 15, 3043–3059, https://doi.org/10.5194/hess-15-3043-2011, 2011.

Schelle, H., Iden, S. C., Fank, J., and Durner, W.: Inverse Estimation of Soil Hydraulic and Root Distribution Parameters from Lysimeter Data, Vadose Zone Journal, 11, vzj2011.0169, https://doi.org/10.2136/vzj2011.0169, 2012.

Schjønning, P., Munkholm, L. J., Moldrup, P., and Jacobsen, O. H.: Modelling soil pore characteristics from measurements of air exchange: The long-term effects of fertilization and crop rotation, European Journal of Soil Science, 53, 331–339, https://doi.org/10.1046/j.1365-2389.2002.00438.x, 2002.

Seneviratne, S. I., Lehner, I., Gurtz, J., Teuling, A. J., Lang, H., Moser, U., Grebner, D., Menzel, L., Schroff, K., Vitvar, T., and Zappa, M.: Swiss prealpine Rietholzbach research catchment and lysimeter: 32 year time series and 2003 drought event, Water Resources Research, 48, https://doi.org/10.1029/2011WR011749, 2012.

Šimůnek, J., Jarvis, N. J., Van Genuchten, M. T., and Gärdenäs, A.: Review and comparison of models for describing non-equilibrium and preferential flow and transport in the vadose zone, Journal of Hydrology, 272, 14–35, https://doi.org/10.1016/S0022-1694(02)00252-4, 2003.

Šimůnek, J., van Genuchten, M. T., and Šejna, M.: Recent Developments and Applications of the HYDRUS Computer Software Packages, Vadose Zone Journal, 15, vzj2016.04.0033, https://doi.org/10.2136/vzj2016.04.0033, 2016.

Skilling, J.: Nested sampling for general Bayesian computation, Bayesian Analysis, 1, 833–860, https://doi.org/10.1214/06-BA127, 2006.

Stumpp, C., Maloszewski, P., Stichler, W., and Fank, J.: Environmental isotope (δ18O) and hydrological data to assess water flow in unsaturated soils planted with different crops: Case study lysimeter station "Wagna" (Austria), Journal of Hydrology, 369, 198–208, https://doi.org/10.1016/j.jhydrol.2009.02.047, 2009.

Stumpp, C., Stichler, W., Kandolf, M., and Šimůnek, J.: Effects of Land Cover and Fertilization Method on Water Flow and Solute Transport in Five Lysimeters: A Long-Term Study Using Stable Water Isotopes, Vadose Zone Journal, 11, https://doi.org/10.2136/vzj2011.0075, 2012.

Taylor, R. G., Scanlon, B., Döll, P., Rodell, M., Van Beek, R., Wada, Y., Longuevergne, L., Leblanc, M., Famiglietti, J. S., Edmunds, M., Konikow, L., Green, T. R., Chen, J., Taniguchi, M., Bierkens, M. F., Macdonald, A., Fan, Y., Maxwell, R. M., Yechieli, Y., Gurdak, J. J., Allen, D. M., Shamsudduha, M., Hiscock, K., Yeh, P. J., Holman, I., and Treidel, H.: Ground water and climate change, Nature Climate Change, 3, 322–329, https://doi.org/10.1038/nclimate1744, 2013.

Taylor, S. A., Ashcroft, G. L., and Others: Physical edaphology. The physics of irrigated and nonirrigated soils., 1972.

Tóth, G., Rman, N., Ágnes, R. S., Kerékgyártó, T., Szocs, T., Lapanje, A., Černák, R., Remsík, A., Schubert, G., and Nádor, A.: Transboundary fresh and thermal groundwater flows in the west part of the Pannonian Basin, Renewable and Sustainable Energy Reviews, 57, 439–454, https://doi.org/10.1016/j.rser.2015.12.021, 2016.

Van Genuchten, M. T.: A closed-form equation for predicting the hydraulic conductivity of unsaturated soils, Soil science society of America journal, 44, 892–898, 1980.

Vereecken, H., Huisman, J. A., Bogena, H., Vanderborght, J., Vrugt, J. A., and Hopmans, J. W.: On the value of soil moisture measurements in vadose zone hydrology: A review, Water Resources Research, 46, https://doi.org/10.1029/2008WR006829, 2008.

Vereecken, H., Schnepf, A., Hopmans, J., Javaux, M., Or, D., Roose, T., Vanderborght, J., Young, M., Amelung, W., Aitkenhead, M., Allison, S., Assouline, S., Baveye, P., Berli, M., Brüggemann, N., Finke, P., Flury, M., Gaiser, T., Govers, G., Ghezzehei, T., Hallett, P., Hendricks Franssen, H., Heppell, J., Horn, R., Huisman, J., Jacques, D., Jonard, F., Kollet, S., Lafolie, F., Lamorski, K., Leitner, D., McBratney, A., Minasny, B., Montzka, C., Nowak, W., Pachepsky, Y., Padarian, J., Romano, N., Roth, K., Rothfuss, Y., Rowe, E., Schwen, A., Šimůnek, J., Tiktak, A., Van Dam, J., van der Zee, S., Vogel, H., Vrugt, J., Wöhling, T., and Young, I.: Modeling Soil Processes: Review, Key Challenges, and New Perspectives, Vadose Zone Journal, 15, vzj2015.09.0131, https://doi.org/10.2136/vzj2015.09.0131, 2016.

Vogel, W.: Österreich - Vorreiter im Grundwasserschutz, Ländlicher Raum, p. 12, 2001.

von Freyberg, J., Moeck, C., and Schirmer, M.: Estimation of groundwater recharge and drought severity with varying model complexity, Journal of Hydrology, 527, 844–857, https://doi.org/10.1016/j.jhydrol.2015.05.025, 2015.

Vrugt, J. A. and Sadegh, M.: Toward diagnostic model calibration and evaluation: Approximate Bayesian computation, Water Resources Research, 49, 4335–4345, https://doi.org/10.1002/wrcr.20354, 2013.

Vrugt, J. A., ter Braak, C. J. F., Clark, M. P., Hyman, J. M., and Robinson, B. A.: Treatment of input uncertainty in hydrologic modeling: Doing hydrology backward with Markov chain Monte Carlo simulation, Water Resources Research, 44, https://doi.org/10.1029/2007wr006720, 2008.

Wang, T., Istanbulluoglu, E., Lenters, J., and Scott, D.: On the role of groundwater and soil texture in the regional water balance: An investigation of the Nebraska Sand Hills, USA, Water Resources Research, 45, https://doi.org/10.1029/2009WR007733, 2009.

Wesseling, J., Elbers, J., Kabat, P., and Van den Broek, B.: SWATRE: Instructions for input, Internal Note, Winand Staring Centre, Wageningen, the Netherlands, 1991, 1991.

Whalley, W. R., Riseley, B., Leeds-Harrison, P. B., Bird, N. R., Leech, P. K., and Adderley, W. P.: Structural differences between bulk and rhizosphere soil, European Journal of Soil Science, 56, 353–360, https://doi.org/10.1111/j.1365-2389.2004.00670.x, 2005.

Wohling, D. L., Leaney, F. W., and Crosbie, R. S.: Deep drainage estimates using multiple linear regression with percent clay content and rainfall, Hydrology and Earth System Sciences, 16, 563–572, https://doi.org/10.5194/hess-16-563-2012, 2012.

Wöhling, T., Vrugt, J. A., and Barkle, G. F.: Comparison of Three Multiobjective Optimization Algorithms for Inverse Modeling of Vadose Zone Hydraulic Properties, Soil Science Society of America Journal, 72, 305–319, https://doi.org/10.2136/sssaj2007.0176, 2008.